To study the corrosion behavior of D-Gun sprayed NiCr coated 347H stainless steel under simulated and actual bio-fuel fired boiler environment

A dissertation submitted
in partial fulfillment of requirements
for the award of degree of

Master of Engineering

in

Production Engineering

Submitted by

HANNAN GADA

Roll No.: 801585010

Under the guidance of

Dr. DEEPA MUDGAL

Assistant Professor

DEPARTMENT OF MECHANICAL ENGINEERING

THAPAR UNIVERSITY

PATIALA (PB), INDIA, 147004

JULY, 2017

Certificate

I hereby declare that the work done in this thesis entitled " **To study the corrosion behavior of D-Gun sprayed NiCr coated 347H stainless steel under simulated and actual bio-fuel fired boiler environment"** submitted towards partial fulfillment of requirement for award of degree of **Master of Engineering** in **Production Engineering, Thapar University, Patiala,** is an authentic record of the work carried out by me under the supervision and guidance of **Dr. Deepa Mudgal,** Assistant Professor, Mechanical Engineering Department, Thapar University, Patiala during 2016 to 2017. No part of the matter embodied in this report has been submitted to any other university or institute for the award of any degree.

Dated: 21-08-2017

Hannan Gada

Registration No.: 801585010

This is to certify that above declaration made by the student concerned is correct to the best of our knowledge and belief.

Acknowledgement

I would like to express my deepest sense of gratitude and a very sincere thanks to my guide **Dr. Deepa Mudgal**, Assistant Professor, Mechanical Engineering Department, Thapar University, Patiala for her sincere and invaluable guidance and full support which helped me in the accomplishment of this dissertation report in present form. Her dynamic and diligent enthusiasm has been highly instrumental in keeping my spirits high. Her flawless and forthright suggestions blended with an innate intelligent application have crowned my task with success. I would like to thank **Dr. S.K. Mohapatra,** Head of Mechanical Engineering Department and all the faculty member and staff members of Mechanical Engineering Department, Thapar University, Patiala for their boundless support.

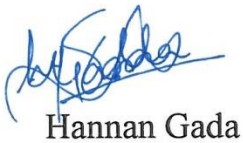

Hannan Gada

Registration No.: 801585010

ME (Production Engineering)

ABSTRACT

High temperature corrosion has lead to failure of different components in field of aerospace, thermal power plants, gas turbines etc. In power generation industries, ferritic and austenitic steels have been used in the high temperature areas because of its ability to withstand at high temperature. However, the current steels are limited to 620ºC. But due to the requirement of increase in efficiency of boiler, the temperature in the boilers is constantly increasing. Moreover, coal is generally used as fuel in the boilers which produces greenhouse gases. Hence, to reduce the problem of green house gases emission, the fuel has been replaced by bio-fuel such as wood, husk etc. Although use of bio-fuel gives lot of advantages such as reduction in green house gases, reduction in fuel cost but burning of such waste can leads to the formation of salt species which can deteriorate the life of the components used in construction of boilers. This can causes unwanted shutdown of the boiler as well as can lead to accidents due to failure of components. To reduce such unwanted shutdown and fatal accidents has lead to purpose of work that is to enhance the corrosion characteristics of 347H SS. It is known that ferritic and martensitic steels that are used in construction of boiler components do not have the required spallation and oxidation properties for boiler tube applications as service temperature of boiler increases. Spallation inside the tube can lead to blockage, overheating, creep rupture and turbine erosion. To obviate these problems austenitic stainless steel grade 347H has been chosen as base metal to carry out the experimentation. 75Ni25Cr coating powder was deposited on 347H austenitic SS sheet by the process of Detonation Gun. Oxidation and hot corrosion studies were done on bare and coated specimens at 800ºC under cyclic condition for 50 cycles. The tests were carried out in laboratory using tubular furnace. Oxidation study was carried out in air whereas hot corrosion study was performed under the simulated bio-fuel fired boiler environment. Mixture of 40%K_2SO_4+10KCl+40%Na_2SO_4+10%NaCl salts were used to simulate the boiler environment. To compare the laboratory test, the samples were also hung in the actual husk fired boiler environment. The boiler was available in Nectar II Company situated at Dera Bassi, Punjab and the temperature inside the boiler was 750C±50C. The samples were hung for 150h duration. Oxidation kinetics was recorded using weight gain technique for laboratory samples. For specimens hung in actual boiler thickness loss measurements were carried out which can help in finding the life of the samples in milli-inches per year. The oxide morphology was characterized using SEM and EDS analysis The bare steel specimen experienced higher weight gain, which

may be due to the formation of protective Cr_2O_3 and unprotective Fe_2O_3 oxide layers in case of samples that were tested in laboratory. Whereas coated samples showed lower weight gain because of the formation of protective Cr_2O_3 and $NiCr_2O_4$ oxide layer. In actual husk fired boiler both the bare and coated samples got intensively corroded. However Ni25Cr coated 347H SS sample was less corroded as compared to bare 347H SS sample.

Table of Contents

Lists of Figures

List of Tables

Acronyms

D-gun	Detonation gun
SEI	Secondary electron image
EDS	Energy dispersive spectroscopy
HVOF	High velocity oxy fuel
Kp	Parabolic rate constant
Min	Minimum
SEM	scanning electron microscopy
XRD	X-ray diffraction
RE	Rare earth
VHN	Vickers hardness number
SS	Stainless steel

CHAPTER 1

INTRODUCTION

1.1 HOT CORROSION/HIGH TEMPERATURE CORROSION

Hot corrosion or high temperature corrosion is a kind of rapid oxidation which attack metal exposed to very high temperature combustion gases having small quantity of certain impurities. Such type of corrosion occurs in those components that are exposed to high temperature like, boilers, gas turbines, jet engines, super heaters and economizers. Fuels that are used in power plants to produce steam contain a large range of impurities in the form of inorganic materials such as sulfates or vanadium compounds that can produce compounds during combustion having low melting points. Such compounds have corrosive nature and can also corrode stainless steel and other alloys which are possessing good corrosion resistance. Another form of high-temperature corrosion includes carbonization, sulfidation and high-temperature oxidation. High temperature corrosion triggered by sulfate is generally categorized into Type I and Type II high temperature corrosion. If the temperature is over the melting points of sodium sulfate then the type of corrosion occurred is called Type I. However if the corrosion occurs below the melting point of sodium sulfate and in the occurrence of small quantity of SO_3 then this type of corrosion is called Type II. During Type I corrosion the protective oxide scale that prevents metal form further oxidation gets dissolved in molten salt and then new protective layer is formed this process repeats causing excessive metal loss. Type II hot corrosion causes formation of small pits with little or no internal attack underneath the protective oxide layer.

When inorganic materials burn in combustion chamber these impurities undergo chemical change by combining with other constituents in the combustion chamber. The effect of such combined materials being formed will depend upon the material properties of component and chemical composition of flue gases that are produced during combustion process. The various effects are

- Corrosion occurred on the wall of furnace.
- Compounds deposited on the super heaters tubes thus reducing boiler efficiency.

- Corrosion occurred in super heaters.
- Air pre-heater plugging.
- Metal loss due to erosion.

1.2 NEED AND AIM OF WORK

High temperature application of components in the area like gas turbines, jet engines and tubes of boilers, superheater and air preheaters require highly corrosion resistant materials. In this project the high temperature corrosion performance of austenitic stainless steels 347H SS was tested in laboratory, and actual boiler environment. As austenitic stainless steel and superalloys are used for construction of components used in temperature area. Efforts were also made to increase the life of the material used in high temperature areas. As thermal spray coating are widely used to deposit on the materials which has been exposed to wear, corrosion and erosion. Hence, in the presence study Ni25Cr coating powder has been deposited on 347H austenitic stainless steel both bare and coated samples were exposed to simulated and actual biofuel fired boiler environment to so as to check its sustainability in such aggressive atmosphere.

1.3 OBJECTIVES OF WORK

In this study the corrosion and oxidation resistance of bare and 75Ni25Cr coated 347H SS austenitic stainless steels were tested properly in laboratory conditions at a temperature of 800ºC and also two samples were extensively examined under actual husk fired boiler. Results were subsequently compared to see if the coated sample provides better protection than bare specimen. Thus the principal focus of this project is to

1) Examine the corrosion and oxidation resistance of coated and bare austenitic steel in air and in corrosive environment by recording spallation and oxide growth activity by exposing these substrates to high temperature (800°C).

2) Study the morphology of oxide layer formed using SEM analysis, EDX analysis and X-ray mapping.

3) Trace the kinetics of oxidation using weight gain analysis.

4) To compare the behavior of bare sample with coated sample in simulated and actual boifuel fired environment.

CHAPTER 2

LITERATURE REVIEW

2.1 INTRODUCTION

Corrosion is a natural occurring process that transforms a pure metal to a chemically stable form, such as its hydroxides, oxides or sulfides (Roberge 2008). It is the slow degradation of metals by some chemical reaction. Naturally metals are not stable and thus tend to convert into compounds which are chemically more stable (Huheey et al. 2006). This process is known corrosion. Corrosion word is derived from the Latin word "corrosus" which means gnawed away (Ekuma and Idenyi 2006). Corrosion engineering is the field connected with preventing and eliminating corrosion.

Most usually corrosion word is used for electrochemical oxidation of metal. (Birks et al 2006). The formation of Fe_2O_3 (rusting) is a case of electrochemical corrosion (Cornell and Schwertmann 2003). This type of corrosion forms salts or oxides of the parent metal which results in a formation of oxide layer that has a reddish orange colorations. Corrosion also occurs in non metals, like in polymers and ceramics (Wang et al. 2006).As ceramic materials posses strong chemical bond between the atoms, that is they have less free energy in there structure. Due to less free energy in there chemical structure ceramic are more naturally stable than metals thus are highly resistant to corrosion.

2.2 DIFFERENT TYPES OF CORROSION

- **Uniform surface corrosion:** This type of corrosion occurs throughout the surface at about the same rate.
- **Pitting corrosion:** This type of corrosion occurs in holes causing increase in hole depth.
- **Shallow pit corrosion:** Corrosion occurs with different rates at different areas.
- **Crevice corrosion:** Local corrosion in connection with crevices occurring in or immediately adjacent to the crevice area, which has developed between the metal surface and another surface (metal or nonmetal).

- **Contact corrosion or dissimilar metal corrosion:** This type of corrosion happens at contact surfaces of two dissimilar metals causing one of the metal to act as anode and other as cathode. Severe corrosion is experienced at anode region.
- **Intergranular corrosion:** This type of corrosion occurs along the gain boundaries of metals.

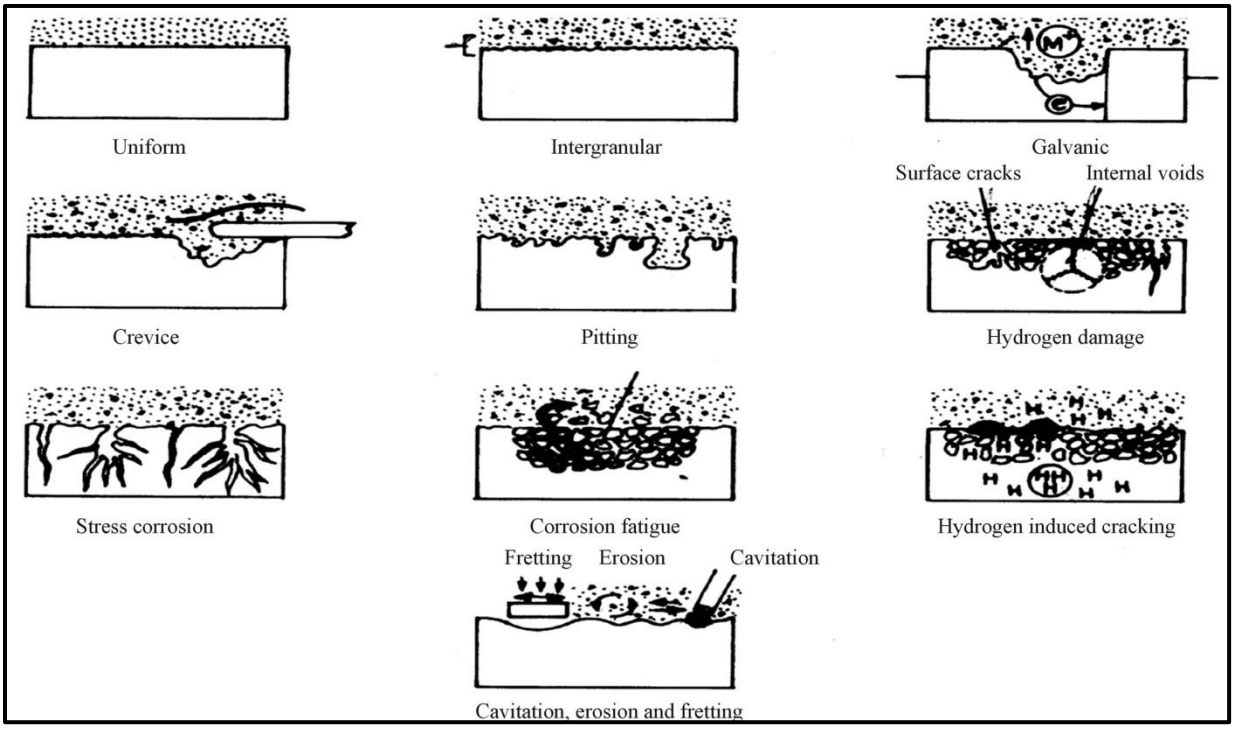

Fig.2.1: Different types of corrosion Mechanism (Anzel 2007)

- **High temperature corrosion/ Hot corrosion:** This is the most aggressive phenomenon of deterioration of alloys, ceramics and metals, when these materials are used at very high temperatures (Stringer 1977). Components that are severely affected by high temperature corrosion are mainly jet engines, gas turbines and industrial plants.

2.3 HIGH TEMPERATURE CORROSION

High temperature corrosion is defined as the accelerated oxidation of materials that is induced by a film deposit of salt at elevated temperatures (Stringer 1977). The fused alkali sulfates are deposited on the hot substrates by the oxidation of heavy metal contaminants like vanadium in

the fuel. High temperature corrosion occur in boilers mainly in two areas water walls and super heaters. At elevated temperatures metals and alloys reacts with its surrounding environment and degrade. This mode of degradation of metals & alloys is called oxidation/dry corrosion. Metals and alloys react with oxygen present in the environment at elevated temperature and form metal oxide layer which may not be dense and adherent enough to stop further oxidation of metal/alloy.

2.3.1 CAUSES OF HOT CORROSION

Hot corrosion in a steam power plants, mostly occurs as a result of the presence of impurities like chlorine, sulphur, and alkali metals. In combusted fuel, the main impurities are chlorine vanadium, sodium, and sulphur (Meadowcroft 1987). In the boiler, these elements join to form various types of compounds. The chemistry of these reactions taking place during combustion is complex and is widely varying. However, all the reactions undergo certain changes that are simple to understand. The sulphur in the fuel combines with oxygen to form sulphur dioxide and trioxide, depending upon the availability and temperature.

Vanadium reacts with oxygen and forms vanadium oxides. Such oxides act as catalysts and coverts sulphur dioxide to sulphur trioxide. In turn sulphur trioxide acts as a catalyst for converting vanadium oxides to vanadium pentoxide. Now this vanadium pentoxides reacts with sodium that is present in the fuel to form sodium metavenadate, which has a low melting point. Vanadium sulphates are also formed during combustion depending on the environment and the amount available in that environment.

Moreover these alkali vanadates and vanadium sulphates condense along the flue gas path in superheaters and reheaters where metal temperatures are in a range for condensation of these types of compounds (Anžel 2007). Depending on the level of temperature of the tubes the vanadates remain as hard deposits that are difficult to remove even by mechanical means. There are different corrosion mechanisms that are believed to happen on tube surfaces and depend on:-

- Local chemistry of deposits.
- Local chemistry of combustion gases.
- Metal compositions.
- Exhaust gas temperature.
- Metal tube temperature.

In nature there is no pure metal that is stable in air at room temperature except for the exception of gold. These metal react with oxygen to form more stable compounds, but the rate at which these reactions occur are very gradual at room temperature. The rate of reaction increases with increase in temperature at very high temperatures most of these reaction are completed in only some minutes (Anžel 2007).So if we are able to understand the reaction rates we may be able to control corrosion problems.

Most Commonly followed laws to measure the kinetics of oxidation calculated by weight change measurements are discussed briefly below:

(a) Cubic Law: Mostly common in experimental studies that a metal/alloy follows at relatively lower temperatures.

(b) Linear Law: In this law, rate of reaction is independent of time. It is followed where the rate of reaction is controlled by diffusion through the gas.

(c) Parabolic Law: In this case, the reaction rate is inversely proportional to the square root of time. Parabolic law is followed where rate of oxidation is defined by diffusion through scale.

(d) Logarithmic Law: It is also followed at lower temperatures generally in the cases where a very thin oxide layer is formed over the surface of substrate under consideration.

2.4 GROWING NEED FOR REDUCING HOT CORROSION

As there is necessity of increasing efficiency of powerplants in order to reduce air pollutants and well as to meet the electricity demand, pressure and temperature of modern powerplants are increased. This has resulted in increasing rate of hot corrosion in different components of powerplant like boilers, economizers, superheater and preheaters. With an increase in powerplant efficiency from 33% to 55% is estimated to decrease carbon dioxide production by 30% (Asbury and Brooks 2007).

Electricity demand of about 74% in UK is fulfilled by non renewable source of energy (38% coal- or oil-fired and 36% gas-fired) (Anzel 2007). Moreover half of the gas-fired powerplants are used as combined cycle (i.e., gas turbine powerplants + steam turbine powerplants), so almost more than 50% of UK electricity generation is directly dependent on steam powerplants (Anzel 2007). However to increase the efficiency of powerplants there is requirement of increasing temperature in boiler. Moreover modern powerplants are designed to use ultra-supercritical steam (temperature more than 565°C and pressure more than 27.5MPa)

that runs on very high temperature and pressure. More Research programmes are conducted such as USC in the US and THERMIE in Europe that are trying to develop system that can handle temperature at 800°C and 35-39 MPa (Blunt and Balchin 2002). Due to such increase in temperature and pressure there is need of materials that will have strong resistance against harsh environment particularly in combustion chamber where temperature is very high like boiler tubes, ecomonizer, and superheater.

There are three main requirements of boiler tubes; proper creep strength, good corrosion resistance and oxidation resistance (Bemer et al. 2010). Such conditions ask for advanced materials that can endure these severe temperature and pressure conditions. Design of such materials is based on creep properties, spallation and oxidation that are important performance properties. Spallation oxide scale causes blockage of steam, reduction in efficiency, over heating of steam. It may also cause sputtered oxide to transport along the tube up to the turbines causing erosion of blades and turbine, resulting in erosion damage (Cornell and Schwertmann 2003). Excessive erosion of tubes could result in loss of load bearing capacity thus causing failure in the system(Grabke et al.1995).Sputtering of oxide layer is mainly cause by difference in coefficient of thermal expansion between pue metal and oxide layer. This temperature variation is caused due to servicing or shutdowns. To minimize the effect of spallation at higher service temperatures these plants should be used for continuous service. For cyclic conditions lower peak service temperatures should be used (Ekuma et al. 2006). The internal stresses are cuased due to difference in thermal expansion coefficients between the different oxide layers that are formed due to oxidation, hot corrosion and the substrate.

Currently use of austenitic steels is done in areas which are exposed to very high temperature like reheaters, ecomizer and superheaters in conventional stations. The occurrence of spallation has been reported in martensitic steels for quite a long time leading to failure in tubes. Recently built powerplants in China which are operating at very high steam temperatures have experienced oxide spallation which had also caused tube blockages (Gupta et al.2012). By increasing service temperature (600º C and upwards) more austenitic stainless steel pipes are been used reheaters and superheater and other components in powerplants. Moreover great importance is being placed on the requirement for oxidation/corrosion resistance over increased mechanical strength. Nowadays higher chromium content stainless steels are being used that enables higher operating temperatures apart from the ferritic/martensitic steels' limit. Hence as

increasing temperature in combustion chamber to attain high steam temperature helps in increasing efficiency of powerplant but also causes increases rate of corrosion.

2.5 BOILERS IN POWERPLANT

A boiler is a fuel burning apparatus that is used for heating liquid mainly water. Boilers are used in thermal power plants to convert water into steam that is used to run turbines for generation of electricity. The vaporized fluid is used for different purposes like

- Power generation
- Cooking and sanitation
- Heating applications

2.6 CLASSIFICATION OF BOILERS

2.6.1 CLASSIFICATION BASED ON CONTENT OF TUBES

- **Fire tube boiler:**-In this a type of a boiler flue gases from the combustion chamber passes through the tubes that are wounded in a sealed box usually containing water. The transfer of heat from the gases to the walls of the tubes occurs by thermal conduction, and then transferred to the water by thermal convection (Baxter 2005).Examples of fire tube boiler include, Cochran boiler, Lancashire boiler, simple vertical type boiler and Locomotive Boiler.
- **Water tube boilers:-**This is a type of boiler in which water circulates in tubes and these tubes are heated externally by the combustion of fuel like Bobcock and Wilcox boiler. Fuel that is being used is combusted inside the furnace which produces hot flue gases that are responsible for converting water into steam (Kakac 1991).

2.6.2 CLASSIFICATION BASED ON STEAM PRESSURE

- **High pressure boilers: -** This type of a boiler produces steam at a pressure 85 kgf/sq.cm or above. Due to production of steam at high pressure this type of boiler is called high pressure boiler. Nowadays high pressure boilers are being

implemented for power production and modern boilers have capacities that are ranging from 40 to 1600 tonnes/hr of superheated steam with a pressure upto 210 kgf/sq.cm and a temperature of about 650'C.

- **Low pressure boilers:-** This type of boiler is used at a pressure below 15psi. These type of boilers were used in past as there efficiency was low. Due to increasing cost of fossil fuel present powerplants are working under high pressure boilers and super critical boilers (Kakac 1991).

2.6.3 TYPE OF WATER CIRCULATION

- **Natural circulation**:- In this type of boiler, water circulation takes place naturally due to difference in density caused when water is heated. Convection currents are set up during heating of water which causes circulation of water in boiler system (Kakac 1991).
- **Forced circulation:-** Water is forced to circulate inside the boiler by using pump. In some cases water is circulated 20 times the rate of evaporation. Examples of forced circulated boilers are Lamont boiler and Clayton boiler.

2.6.4 FURNANCE POSITION

- **Externally fired**:- These type of boilers have separate furnace where fuel is combusted. Usually the furnance is below the boiler shell (Gurumoorthi etal. 2008). The horizontal return tube (HRT) boiler is the most extensively used external boiler.
- **Internally fired:-** In this type of boiler the furnace is a fundamental part of the boilers structure (Watanabe et al. 2000).The scotch marine boilers, vertical tubular and locomotive are some examples of internally fired boiler.

2.6.5 TYPES OF FUEL USED

- **Coal Fired:-** In this type of boiler coal is used as a fuel. These types of boiler are used for generation of electricity in thermal power plants. Nowadays mostly

pulverized coal is used for power generation and is responsible for producing thermal energy that helps in generating 50% of worlds electricity.

- **Oil Fired:-**When liquid fuels are used in boilers to produce steam then those boilers are called as oil fired boilers. These type of boilers are the used in the countries with abundance of petroleum reserves, such as the gulf countries.
- **Gas fired:-** These boilers burn gases to produce necessary heat for production of steam in powerplant. In gas boilers natural gas or propane is most commonly used. Use of propane or natural gas depends upon the availability of these fuels. In USA propane is available in almost all states of country. However on the other hand natural gas is less expensive as compared to propane.

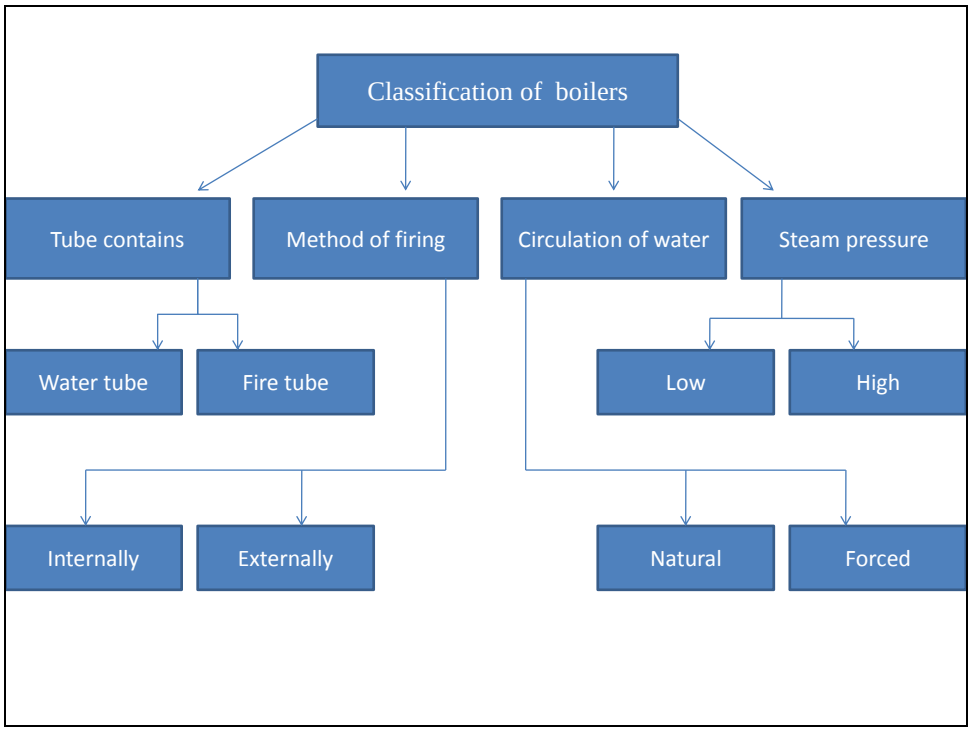

Fig 2.2: Classification of Boilers

2.7 THERMAL SPRAY PROCESS

In this coating process, where the material that is to be coated is melted by flame, electric arc, plasma arc or any other technique to a semi-molten or molten state after that semi-molten or

molten state material is propelled towards the bass metal by different processes. Subsequent sprayed particles build up to form the coating with the lamillnar structure (Paulussen et al. 2005).

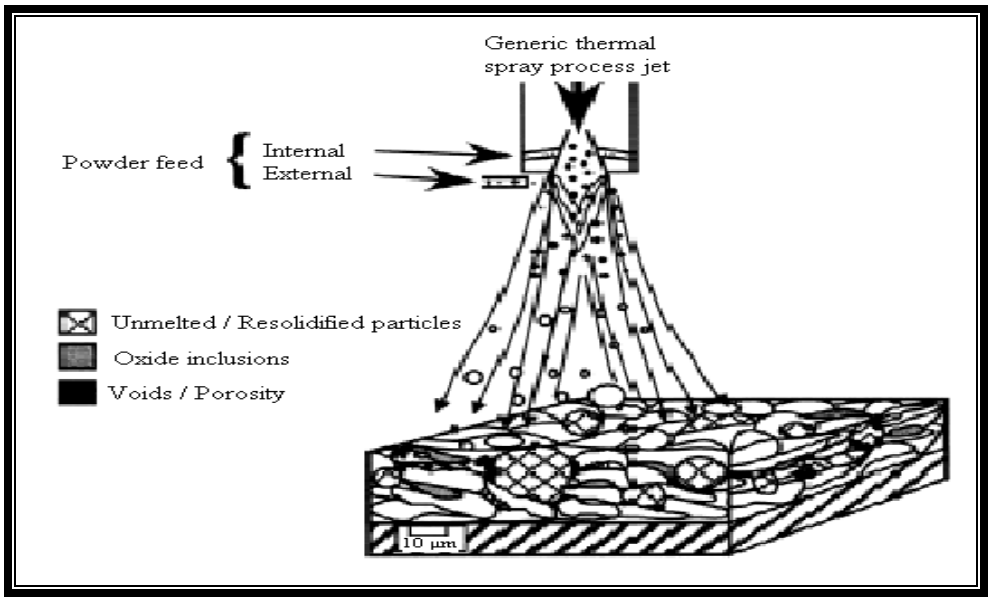

Fig 2.3: Process illustration of thermal spray technique (Davis JR 2004)

2.8 CLASSIFICATION OF THERMAL SPRAYING

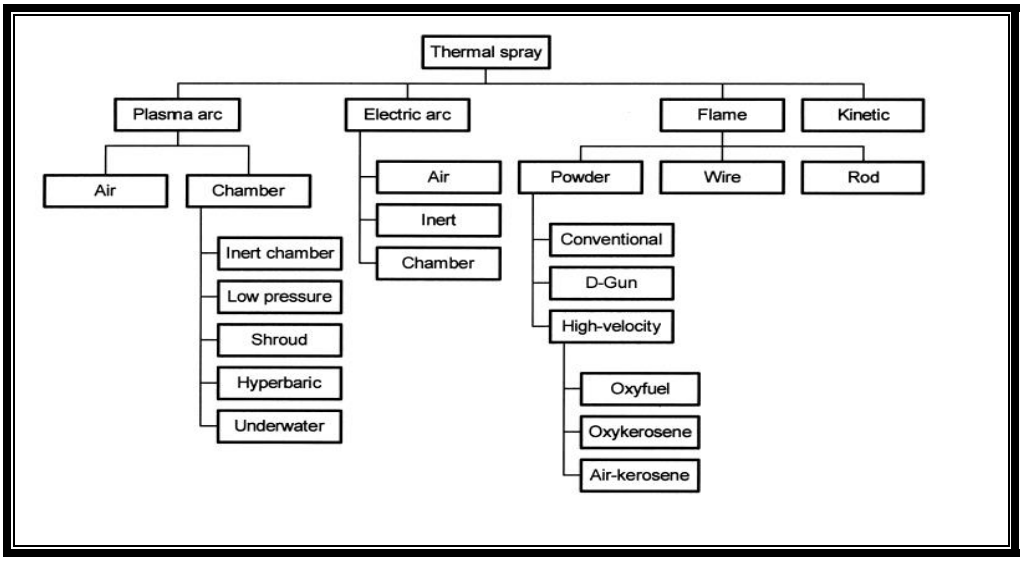

Fig 2.4: Classification of thermal spray techniques (Davis JR 2004)

2.8.1 WIRE ARC SPRAYING

It is a thermal spraying technique where two consumable metal wires are fed into the spray gun. Then these wires are charged to establish an arc and heat from this arc melts the incoming wire, which is then carried by air jet from the gun (Kuroda et al. 2008). This molten metal is then deposited onto a substrate by using compressed air. This technique is typically used for heavy and metallic coatings.

2.8.2 WARM SPRAYING

This process is a alteration of HVOF spraying technique. In this technique nitrogen is mixed with combustion gas in order to reduce the temperature of combusted gas. Doing so helps in bringing the process closer to the cold spraying. The combusted gas contains unreacted hydrocarbons, oxygen and water vapours (Kawakita et al. 2008).The coating efficiency is higher than cold spraying. As the coating is deposited at low temperature this helps to reduce reaction chemical reaction that occur at high temperature between coating and surrounding environment. This type of coating technique is usually used for plastics, metallic glasses and Titanium (Kuroda et al. 2008).

2.8.3 COLD SPRAYING

In this technique, converging–diverging de Laval type nozzle is used to accelerate the particles to very high speeds. Particles are carried to substrate with the help of carrier gas. Upon impact of these particles with substrate, particles deform plastically as there is enough kinetic energy and then adhere mechanically to the surface to form a coating (Hussain et al 2009). The critical velocity that is required to plastically deform coating material on impact depends upon various material properties like, temperature and powder size. Composite materials and nanocrystalline powders, Polymers, metals and ceramics can be coated on substrate by using cold spraying (Leroux et al. 2008)Metals such as Al and Cu are best suited for cold spraying as they are soft, but coating of hard materials (Ta, W, Ti, WC–Co, MCrAlY etc.) by cold spraying has been reported (Kuroda et al. 2008).

2.8.4 DETONATION GUN

Detonation gun is also called D-gun. It is consists of a long water-cooled barrel with inlet valves for gases and powder. Fuel (acetylene most commonly used) and oxygen are fed into the barrel along with a powder that is to be coated on substrate. Spark is used to burns fuel mixture and the resulting detonation is used to melt and accelerates the coating powder to a supersonic speed through the barrel (Tanner CB 2008). Nitrogen gas passed through the barrel after each detonation to keep the barrel clean. The whole process takes place in less than a second. The molten and semi molten particles are suspended in combusted gas and on impact these partiles form strong and dense coating.

2.9 STUDIES DONE UNDER BOILERS

Kamal et al. (2008) carried out hot corrosion studies under the molten salt 75 wt.% Na_2SO_4+25 wt.% K_2SO_4. The environment is generally formed while burning the waste material in the boiler furnace. As this salt has low eutectic point, hence the salt can melt and dissolve the protective oxide formed on the alloys. The temperature chosen for hot corrosion was 900°C. The studies were carried out under cyclic condition. Cr_3C_2-NiCr coating was deposited using Detonation gun process on three different superalloys Superfer 800H, Superni 75 and Superni 718. The corrosion tests were done to compare the corrosion resistance of bare and coated alloys under aggressive atmosphere. All the coated alloys performed satisfactorily by forming two different types of oxide having chromium and nickel content. All the three coated alloys also showed lower weight gain a compared to bare samples thereby showing the better resistance to corrosion. Out of all the three coated superalloys, Cr_3C_2-NiCr coated Superfer 800H provides least corrosion resistance.

Mahesh et al. (2008) performed corrosion test on NiCrAl coated Ni- and Fe-based superalloy substrates. The coating was deposited using HVOF thermal spray process. Molten salt environment produces due to residual oil (Na_2SO_4–60% V_2O_5) was selected to carry out the corrosion study. The temperature chosen was 900°C. It was found that the elements such as chromium, aluminum, nickel helps in providing good corrosion resistance to the coated alloys as these elements have tendency to form protective oxide when exposed to high temperature.

Zhou et al. (2016) again carried corrosion studies under the boiler environment. For this HVOF process was used to deposited the coating. Sintered and agglomerated Cr_3C_2- NiCrMoNbAl

coating powder was used to deposit on P91 boiler steel. Cr_3C_2-is the hard phase (Cr_3C_2) of the coating system and and (NiCrMoNbAl) act as a matrix for the system. This coating system is used as it meets the requirement of harsh environment which occurs due to wear, corrosion, high temperature in the boilers. The test was conducted for bare, Cr_3C_2-NiCr and Cr_3C_2-NiCrMoNbAl coated P91 steel so as to compare the corrosion resistance of all the three specimens. Among all the three specimens, Cr_3C_2 -NiCrMoNbAl coating shows excellent corrosion resistance. As no major spallation was observed in case of Cr_3C_2 -NiCrMoNbAl coating. The higher corrosion resistance of this particular alloy might have occurred due to the elements present in the coating which effectively formed the protective oxides during corrosion run.

Sidhu et al. (2008) evaluated the HVOF sprayed WC-NiCrFeSiB coated on Superfer 800H and Superni 75 under the hot corrosion and oxidation environment. The specimens have been kept under the molten salt (Na_2SO_4-25%NaCl) environment and in air at 800°C under cyclic conditions. The salt environment again simulates the environment present in boilers used to burn waste. WC-NiCrFeSiB coating successfully protects the two different superalloys that are nickel based and iron based which has been used to carry out the study. Chromium and nickel mainly contribute in providing lower corrosion rate by forming oxide. Also, these oxides were formed along the splats boundaries also. As oxygen is generally entrapped during the coating deposition particularly along the splats boundaries.

Aho et al. (2009) investigates the effect of adding sulphates of aluminium and iron in processes producing sewage sludge (SWS). This has been done to avoid the deposition of chlorine and to destroy the alkali chlorides. Digested and raw sewage sludge were mixed with a fuel containing bark and recycled fuel (REF). However chlorine content was effectively decreased when biomass feedstock was added in sewage sludge. Also the alkali sulphates found in the fine fly ash confirmed the contribution of sulphation to alkali capture.

Chatha et al. (2012) conducted as study to evaluate the hot corrosion behavior of bare and (HVOF) sprayed Cr_3C_2–NiCr coated T91 boiler steel. Heat treatment and sealing of the deposited coating has also being carried out as post treatment. Molten salt corrosion test under Na_2SO_4–60% V_2O_5 salts were carried out to check the performance of the post treatment of the coating. The studies were conducted at 900°C under non-isothermal conditions. Coated steel showed better resistance to hot corrosion as compared to the bare T91 steel. Coated sample underwent two stages of hot corrosion, viz. initiation stage and propagation stage. When coating

entered the propagation stage, the protective oxide layer became ineffective and thus substrate was vulnerable to hot corrosion. Post treated coated T91 sample showed better resistance to hot corrosion than simply coated T91 sample.

Szymanski et al. (2014) reported that thermal spray processes were used in the power plant industries against the corrosion, erosion and wear prone areas. In Poland, problems that have been encountered while fabricating the coatings using thermal spray process and also the material used were analyzed carefully. The techniques used for spraying coating by thermal spray were characterized. This can helps in depositing the coating with appropriate coating for functional performance with respect to the phase structure, chemical composition and various other properties.

Reddy et al. (2006) carried out the hot corrosion studies on two dissimilar weldments under Na_2SO_4+V_2O_5 (60%) environment at 500 to 600°C under cyclic condition. Friction welded process was used to weld the two different steel that is AISI 4140 and AISI 304. Surface analytical techniques were used to characterize the oxide scales formed in the weldment. It was concluded that low alloy steel suffered from spallation along with the formation of thick oxide. Moreover it was observed that the weldment area is more prone to corrosion in comparison to the two base steels.

Kumar et al. (2007) studied the effect of molten salt Na_2SO_4-60% V_2O_5 environment on different region of tungsten inert gas welded T22 boiler tube steel. The studies were conducted at 900°C. The thick oxide layer was formed on HAZ region along with the formation of coarse grain bainite. The base metal suffered from high corrosion rate followed by HAZ region and weld metal.

Singh et al. (2012) explained the advantage of using detonation gun thermal process by providing information related to the has flow rate and particle velocities. It was reported that this process is capable of achieving very high particles velocities and gas flow rate. A part from this, the coating so developed has very high bond strength and hardness. The technique is useful for depositing various types of coatings including ceramic, cermet and metallic. Hence, a oxidation study was carried out on Cr_3C_2–NiCr coating on T22 boiler steel. This coating was exposed to high-temperature oxidation in air and oxidation erosion in actual boiler environment at 700±10°C under cyclic condition. It was reported that Cr_3C_2–NiCr coating was successful in proving the protection to the bare steel. T91 steel suffered from intense spalling along with the

higher weight gain during oxidation. Whereas, coating remains adherent with the substrate throughout the cyclic process in laboratory level as well as in actual boiler environment. The steel suffered from higher weight loss as compared to its coated counterpart. Main oxide which was formed on the coating was chromium oxide which helps in protecting the coated substrate.

2.10 LITERATURE GAP

As of the above literature it can be summed up that the application of the coatings on the heat facing surfaces of component might provide better protection in harsh atmosphere at high temperatures. Therefore in present work , bare and NiCr coated 347H SS have been subjected to simulated husk fired boiler environment (Na_2SO_4-NaCl-K_2SO_4-KCl and Na_2SO_4-25NaCl) at 800°C for 50 hour (1hour heating 20 minutes cooling) under cyclic condition in laboratory. NiCr coating was applied on 347H SS substrates by using detonation gun process. The coated as well as bare 347H SS specimen were subjected to high temperature corrosion test that were conducted in air and also under simulated atmosphere at 800°C for 50 cycles. The molten salt environments selected in the present study may simulate the environment present in the boifuel fired boiler. The mixer of salts present form a low melting eutectics which are high corrosive in nature. As no study has been reported in which the corrosion behavior of these samples were evaluated under bio-fuel fired atmosphere. Therefore, the present research work is envisaged to make a detailed investigation of Detonation Gun sprayed coatings on 347H SS subjected to oxidation, hot corrosion and also in actual boiler environment.

To compare the study, the corrosion test were also conducted in actual boiler environment. Husk fired boiler running at 750ºC was chosen for the study. Both bare and coated 347H SS was exposed to actual boiler atmosphere for 150 hours. No study has been carried out to check the corrosion performance of bare 347H stainless steel under husk fired boiler atmosphere.

CHAPTER 3

EXPERIMENTATION

3.1 INTRODUCTION

Three studies were carried out for this paper; Oxidation and Hot corrosion under simulated conditions prepared in laboratory and in actual boiler environment. For oxidation and hot corrosion studies were conducted in laboratory, there were some common equipment used i.e a digital weighing balance, tubular furnace and alumina boats and a tong. Digital weighing balance having a least count of 0.0001 was used to carry out weight gain analysis. Maximum temperature of the tubular furnace was 1200°C and the experiment was conducted at 800°C under cyclic conditions. In actual boiler environment conditions the specimens were suspended in actual husk fired boiler near super heater tubes. Maximum temperature recorded near super heater tubes was 800ºC that was calculated by pyrometer used in the plant and average temperature range lie between 750±50ºC

3.2 SUBSTRATE MATERIAL

In metallurgy, stainless steel is also known as inox or inox steel. Stainless steel finds its application typically in areas where there is a requirement of good corrosion resistance. Food handling and cutlery are among those other applications.

347H offers an excellent resistance to corrosion following exposure to temperatures from 800 to 1500°F (427 to 816°C). Besides having a good corrosion resistance, it is also practical for high temperature service because of its good mechanical properties. It provides a good creep strength and oxidation resistance till temperature of 1500°F (816°C). In this temperature range, the overall corrosion resistance of 347H stainless steel plate is superior to 321 stainless steel plate. It also performs somewhat better than 321 SS in strongly oxidizing environments up to 1500°F (816°C).

Table 3.1: Chemical composition of SS 347H

Elements	SS 347
Chromium	17.00 min.-19.00 max.
Nickel	9.00 min.-13.00 max.
Carbon	0.04 min.-0.10 max.
Manganese	2.00
Phosphorus	0.045
Sulfur	0.03
Silicon	0.75
Columbium & Tantalum	10 x (C + N) min.-1.00 max.
Iron	Balance

3.2.1 SUBSTRATE PREPARATION

Ni and Cr based super alloy 347H SS have been used in present investigations which were procured from Cheema Boilers, (Derrabassi), Punjab, India. The specimens of size 20x15x5(mm) have been cut from' the sheet using EDM process. After that these substrates were polished using 220, 320, 600, 1000, 1200 and 2000 grit size emery paper. Then these substrates were cloth polished using alumina powder of 0.1micron. After surface polishing the samples were cleaned by acetone to remove any contamination Then these samples were grit blasted with alumina having grit size 20 microns to increase surface roughness so that to improve bond strength between coating and substrate. After grit blasting the sample were coated using detonation gun.

Fig 3.1: Image of detonation gun apparatus.(courtesy SVX company Greater Noida)

Figure 3.2: Control panel of Detonation gun spray process (courtesy SVX Company Greater Noida UP)

3.2.2 FEEDSTOCK MATERIAL USED FOR COATINGS

Commercially available Nickel-Chromium (75Ni25Cr) powder has been used for depositing on the specimens. The chemical composition and particles size of the coating powder is given in Table.3.2.

Table 3.2: Composition of coating powder size of the particles

Coating Powder	Chemical Composition	Shape	Particle size
NiCr	75Ni-25Cr	Spherical	10-45μm

3.2.3 COATING FORMULATION

347H SS having composition 17-19% Cr 9-13% Ni 0.08C 2%Mn 0.75% Si 0.045%P 0.030S was procured from Cheema Boilers located at Ropar Punjab in the form of sheet. Six samples of 347H SS were cut down from the sheet having dimension 15mmx20mm. Thickness of the samples have been reduced to 5mm .The samples were grit blasted before application of coating in order to enhance the surface roughness for better bond strength. Commercially available 75Ni25Cr was deposited on 347H SS substrate. 200-250 μm thick coating was deposited using D-gun technique. The coating was deposited at SVX Powder M surface Engineering, Noida, India. In the table listed below are the various parameters used during the coating process. The consistencies of these parameters were maintained during the entire coating process.

Table 3.3: Parameters of D-gun during application of coating on 347H SS substrate.

Parameters	Details
Working Gases	Oxygen, Acetylene, Nitrogen, Air
Pressure of working Gases (MPa)	
Oxygen	0.2
Acetylene	0.14
Nitrogen	0.4
Air	0.4
Consumption of gases/shot	
Oxygen	27×10^{-5} m^3
Acetylene	23×10^{-5} m^3
Nitrogen	5×10^{-5} m^3
Air	5×10^{-5} m^3
Water consumption rate	15-25 lit/min
Firing rate	1-10 Hz
System control	Manual/ Semi-auto
Sound Pressure level	150 dB
Relative humidity of ambient air	50%

3.2.4 COATING THICKNESS

The thickness of the coating was monitored during the process of D-gun spraying with a coating thickness gauge meter (with precision 1µm) to obtain the coating with uniform thickness. The thichness measured by thickness gauge meter was in range of 200-150µm.

3.3 CHARACTERIZATION OF SAMPLES

3.3.1 SEM ANALYSIS

The surface morphology of chips produced by LSEM has been investigated by scanning electron microscope model JSM-6510LV. The SEM images were taken at 500x, 1000x and 5000X resolution. The effect of feed and speed on surface quality of AL5052 chips produced by different rake angles.

Figure 3.3: Scanning electron Microscope
(Courtesy: SAI Lab, Thapar University, Patiala)

3.3.2 ENERGY DISPERSIVE SPECTROSCOPY

EDS analysis for the specimens was done using EDS (OXFORD, X-Max) with variation of ± 0.3 at. % for heavy elements and ± 2 at.% for light elements software INCA attached with scanning electron microscope. The EDS genesis software indicates the oxides present at a point along with their compositions (weight %). EDS analysis is based on ASTM-E1508-12a standard.

3.3.3 MICROHARDNESS

Micro hardness analysis was done to measure the penetration resistance of the specimen. The surface roughness test was done at Thapar University, Patiala using surface Roughness tester

machine that was made by Mitutoyo (Japan). The least count of surface tester machine that was used for measurement was 0.01μm.

Fig 3.4: Micro hardness testing machine

(Courtesy: Mechanical Workshop, Thapar University)

3.3.4 SURFACE ROUGHNESS TESTER

To determine the surface roughness of specimens, surface roughness tester was used. The Surface Roughness test was done at Thapar University, Patiala. The Surface Roughness tester machine was made by Mitutoyo (Japan). 0.01μm is the least count of the Surface roughness. It is calibrate by the vertical deviations of a real surface from its ideal form. If the deviations are broad, then this mean the surface is rough; if these deviation are less then the surface is smooth.

Roughness is typically considered to be the, short wavelength, high frequency component of a measured surface. Surface roughness is generally a good predictor of the performance of a mechanical component.

Fig 3.5: Surface roughness tester
(Courtesy: Metrology Lab, Thapar University, Patiala)

3.3.5 X-RAY DIFFRACTION

X-ray diffraction (XRD) analysis was performed in order to examine the phases and various compounds that were formed during the experimentation at a particular areas of the specimen. XRD analysis was carried out for the NiCr coated 347H SS and bare 347H SS substrates to determine the various phases present on their surfaces. The substrates were scanned in 2θ range

of 20º to 80º and the intensities were recorded. This analysis is done for determination of various phases with the help of JCPDS cards and X–pert hi score.

Fig 3.6: X-RAY Diffraction

(Courtesy: SAI Lab, Thapar University, Patiala)

3.3.6 CROSS SECTIONAL ANALYSIS

For cross sectional analysis, the samples that were put under oxidation and hot corrosion test were cut vertically using EDM wire cut and then mounted in epoxy resin that was surrounded by PVC pipe to provide required strength during epoxy setting time. These substrates were then polished by using 220,600 and 1000 emery papers followed by alumina cloth polishing. Samples were polished in order to remove excessive epoxy on the substrates surface. After polishing, these samples were gold coated so that these samples become conductive for SEM analysis.

3.3.7 X-RAY MAPPING

To obtain cross sectional analysis of the different elements present in the coatings, the specimens were cut along the cross-section, mounted and polished in accordance with the procedure already discussed in section in 3.3.1. Thereafter the silver pasted was applied from the samples till the

edge of the stub in turn to have conductivity, thereafter; the specimens were gold coated to assist elemental X-ray mapping analysis of the different elements present across the cross section of coated specimens. The chosen area has three different regions i.e. substrate, coating and some epoxy region. X-ray mappings were acquired for all the elements present in the substrate and the coatings but only those mappings are reported which indicates the presence of some elements.

3.4 HIGH TEMPERATURE OXIDATION AND HOT CORROSION STUDIES.

3.4.1 EXPERIMENTAL SETUP

Silicon carbide tubular furnace with PID controller controlled with ±1°C accuracy was used for oxidation and hot corrosion test. Digital vernier caliper was used to note the dimension of each specimen before the start of test. The sample was kept in alumina boats and weight was recorded. These boats were then placed inside the silicon carbide tubular furnace for 1 hour at 800˚C. After 1hour of heating these samples were then taken out and cooled in room temperature for 20 mins. Then these boats were weighted using digital weighing balance and then placed back into the furnance for another cycle. After each cycle the weight of boats were measured.

3.4.2 OXIDATION STUDIES CARRIED OUT IN AIR

The oxidation tests at 800°C were performed on bare and 75Ni25Cr coated 347H stainless steel in laboratory furnace up-to 50 cycles. The samples were kept in alumina boats during experimentation. Boats were heated for 2 hours at 1000°C so as to make the weight of boats constant prior to experimentation. The samples were kept inside the tubular furnace at 800C for 1 hour and after that these samples were taken out and cooled for 30 mins in ambient air. After cooling of specimens then boats were weighted using digital weighing balance. Such 50 cycles were completed and weight gain measurements were recorded. This weight measurement has been taken after every cycle.

3.4.3 HOT CORROSION STUDIES IN SALT ENVIRONMENT

The only difference is that we apply salt solution on specimen before we conduct the test. Salt solution was prepared by mixing K_2SO_4, Na_2SO_4, KCl, NaCl (40:40:10:10 ratio) and distilled water. This salt solution was applied on specimens by using small Camel brush. After the application of salt solution on specimens rest of the test was conducted in similar manner as that of oxidation.

3.4.4 CORROSION STUDIES IN ACTUAL HUSK FUELED BOILER ENVIRONMENT

Biomass has become most widely used source of energy fuel. This is because of the limited availability of non-renewable source of energy such as fossil fuels. Burning of fossil fuel also causes production of green house gases. Hence, biomass such as agricultural residues and wood wastes becomes a viable substitute fuel in electricity generation units (Yoon *et al.* 2012) (Arbon 2002). As reduction in green house gases is one of the biggest advantages of using biomass fuel (Demirbas 2005) (Oliveira *et al.* 2012). Moreover, co-combustion of Biomass-coal also represents a sustainable, low-risk, low-cost, renewable energy option that assured net reduction in SOx and often NOx and CO_2 emissions (Baxter 2005) .

Rice husk is one of the bio-fuel which is being extensively used as a boiler fuel in power boilers as well as different processing industries. It is as excellent fuel with 3,000 kcal per kg of heating value (calorific value) (Web references 1). However, burning of husk produces lot of salt deposits which can contaminate the environment of the boiler. These salt species get deposited on the surface of the components used in the boilers. These deposits then react with the metal oxide formed on the components. Reactions may cause the degradation of the oxide layer by dissolving it. Due to these reactions, the oxide layer will again form on the surface thus consuming the elements present in the component. This will further reduce the life of the component. Hence, some external protection is required to protect the component for longer hours.

To obviate this problem, the experiments have been carried out in actual husk fired boiler environment operating at 750°C for 48h. Austenitic steel 347H has been chosen for the studies as the super heater tubes installed in the boiler is made up of this particular steel. Then, two

different coating were deposited on the surface of the steel using detonation gun technique. A hole was drilled in all the three substrates. All the three samples were hung inside the boiler for 48 working hours using khanthal wire A grade. The exposed samples were then characterize using SEM/EDS and XRD analysis.

3.5 ANALYSIS OF CORROSION PRODUCTS OF OXIDATION AND HOT CORROSION.

3.5.1 VISUAL INSPECTION

Subsequent to every cycle of oxidation and hot corrosion run, oxide layer formed on each substrate was visually examined. This type of inspection helps in deterring the various changes in colour, luster and amount of spallation that occur during different cycles. It also tends to better understanding of development of cracks if any that have occurred during experimentation.

3.5.2 WEIGHT GAIN MEASUREMENTS

The weight change values were measured at the end of each cycle to know the corrosion kinetics after oxidation and hot corrosion. The weight change was measured using digital weighing balance of 0.1mg accuracy. The weight change data was plotted with respect to number of cycles for each specimen and the plots are given in subsequent chapters. However in the case of actual boiler environment conducted study, weight gain measurement were not possible as the specimens were suspended in boiler and amount of spalled matter from specimens combined with boiler ash.

CHAPTER 4

CHARACTERIZATION OF COATING

4.1 NiCr COATING

NiCr coating powder is usually used as the coating materials as it possess some important properties such as erosion resistance, wear resistance, corrosion resistance, and good thermal conductivity. As a result of these properties, NiCr coating is used for coating boiler tubes. Moreover the nanostructured Ni-Cr coatings acquire lesser porosity and improved grain boundary diffusion which helps in formation of denser Cr_2O_3 corrosion protective oxide scale.

4.2 MORPHOLOGY OF POWDER

Surface morphology of 75Ni25Cr coating powder has been shown in fig (4.1). Commercially available 75Ni25Cr powder has been used in the study. The morphology of the powder is shown in Fig (4.1). The particles have spherical structure with in nickel chromium matrix. The particles are embedded within each other. The particle size was found to be in range of 10-45μm.

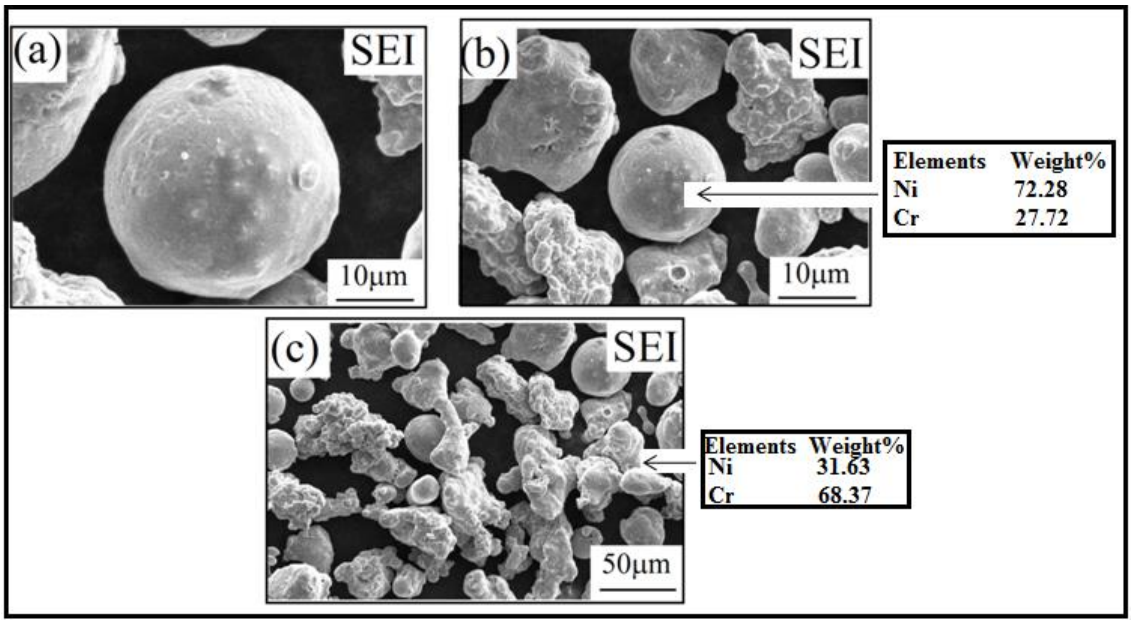

Fig 4.1: SEM images of 75Ni25Cr coating powder under (a) 2000x (b) 1000x (c) 500x

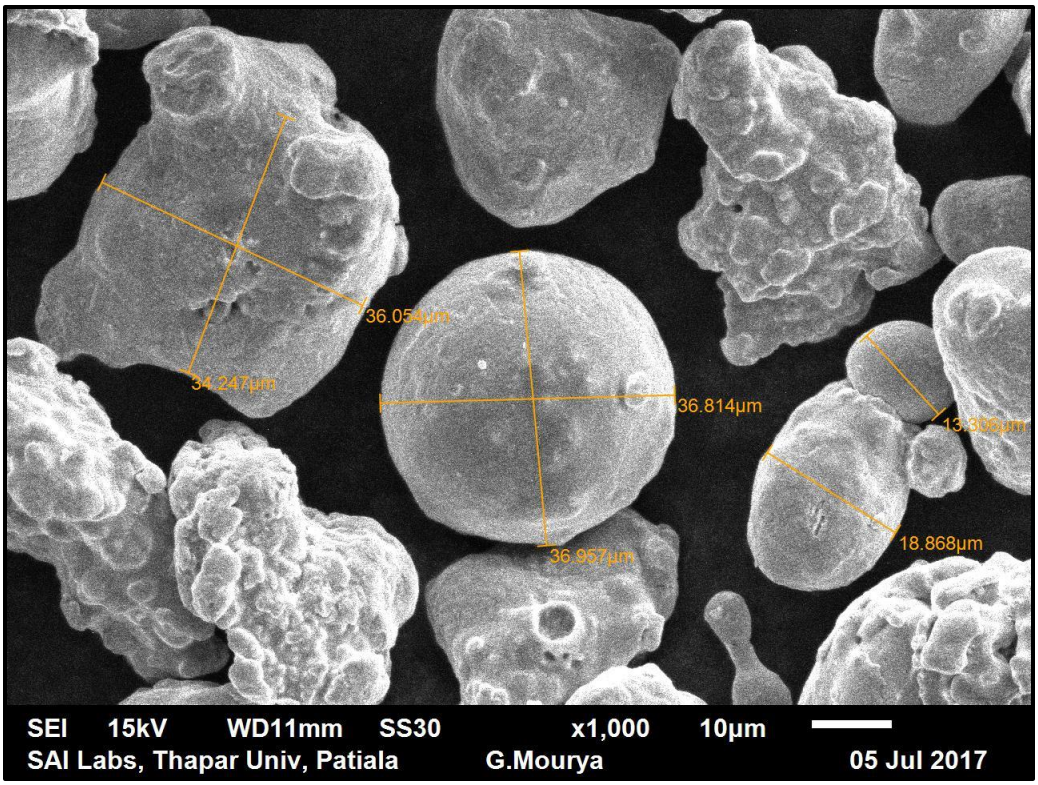

Fig 4.2: SEM image showing powder diameter.

4.3 MICRO HARDNESS TEST

Micro hardness test is carried out to know the hardness of the material. It is used as a standard method for measuring the hardness of metals, in particular, those with extremely hard surfaces. In this process, Standard pressure applied on the surface of the substrate, a pyramid shaped type of indentation seen on the surface of sample by the microscope. The diagonal of the resulting indention is measured under a microscope and a conversion table reads the corresponding Vickers Hardness. Vickers test is performed by placing the specimen on an anvil that has a screw threaded base. The indenter is thereafter pressed into the sample by an accurately controlled test force. The force is maintained for a specific dwell time, normally 20 seconds. After the completion of the dwell time, the indenter is removed and an indent is seen in the surface of the sample in the form of square shaped pyramid. The size of the indent is determined optically by measuring the two diagonals of the square indent. The average of the two diagonals is used in the following formula to calculate the Vickers hardness. The operation of applying and removing the

load is controlled automatically. Several loadings give practically identical hardness numbers on uniform material, which is much better than the arbitrary changing of scale with the other hardness machines. In case of an indentation with a tolerance of ±1/1000 of a millimeter, a microscope is used to measure the square indentation. Finally, an average is taken of all the measurements across all the diagonals. Micro hardness test is performed on the uncorroded NiCr coated steel. Test Vickers No. for NiCr coated 347H SS was found to be 290.53. More the Vickers no. more the hardness of the material. Micro hardness test machine is available at Thapar university Patiala .

4.4 SURFACE ROUGHNESS

Surface roughness can be defined as the shorter frequency of real surfaces relative to the troughs. It can be noticed in various machine parts, that their surfaces embodies a complex design constituting of a series of peaks and troughs of different height, depth and spacing. Surface roughness can also be greatly affected by the microscopic asperity of the surface of each part. The roughness values (R_a) of 75Ni25Cr coated steel was recorded to be 5.05.

4.5 THICKNESS LOSS MEASUREMENTS

The thickness loss is a means to express the penetration rate due to corrosion of the metal specimen. Perhaps the most common unit of corrosion penetration recognized in the United States is milli-inches per year (mpy). The formula utilized to convert mass loss or thickness loss to corrosion rate, in mpy, is as follows:

$$Corroson\ Rate\ ,\ mpy = \frac{(Mass\ Loss, g) \times 3450000}{8760 \times SA \times d} = \frac{(Thickness\ Loss, microns)}{25.4}$$

Where, SA is the surface area in cm^2, and d is the density in g/cm^3.

The calculation of mpy can also be done as follows: In a year there are 8730 hours and 1mm is equal to 39.37 mils. So, for “z” mm thickness loss for 1000 hours, mpy is (z) × (39.37) × (8760/1000).

4.6 MICROSTRUCTURE OF ASPRAYED NiCr COATED AND BARE 347H STAINLESS STEEL

Before examining the specimen by SEM, polishing of sample was done by using emery paper with grit size of 220,400 and 800.followed by alumina cloth polishing. Fig 4.3 shows the morphology of polished bare 347H SS. However fig (4.4) shows the surface morphology of asprayed NiCr coated 347H stainless steel.

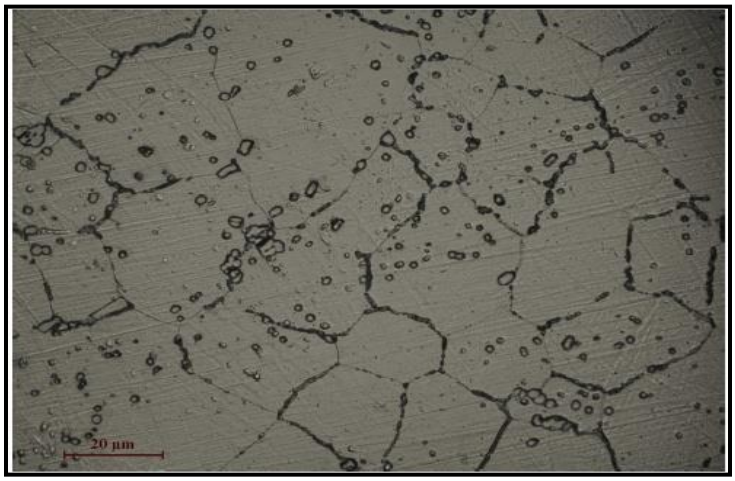

Fig. 4.3 SEM micrograph showing surface morphology of polished bare 347H SS.

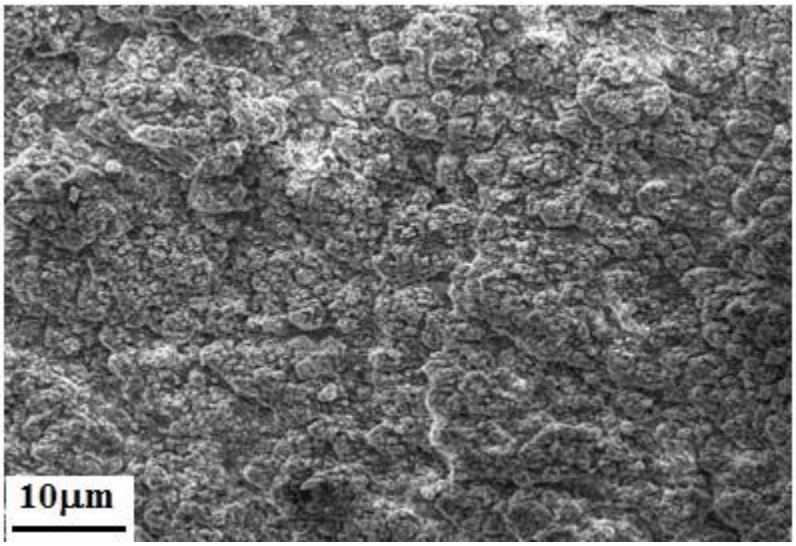

Fig 4.4: SEM micrograph showing surface morphology of Detonation gun as-sprayed NiCr coating on347H Stainless steel.

CHAPTER 5

OXIDATION STUDIES IN AIR

5.1 OXIDATION OF BARE STAINLESS STEEL

5.1.1 RESULTS

5.1.1.1 VISUAL ANALYSIS

Macrophotos of bare 347H SS and 75Ni25Cr coated 347H SS after 1st cycle , 15th cycle and 50th cycle of oxidation at 800°C has been shown in fig 5.1 and 5.2 respectively. In case of bare 347H steel, it was observed that reddish oxide with dark grey background was formed just after 1st cycle (fig. 5.1(b)) of oxidation. After 5th cycle of oxidation, reddish oxide disappeared and dark grey oxide was formed on the surface. No further changes were seen till 50th cycles (fig.5.1(d)). On the other hand light greenish oxide was formed on the surface of Ni-25Cr coated 347H just after 1st cycle (fig. 5.2(a)) of oxidation and remained till 5th cycle. After 6th cycle, it was observed that dark grey oxide was formed on the surface which does not change till 50th cycle (fig.5.2(d)). Minor amount spallation was observed throughout the experiment in case of bare sample.

5.1.1.2 WEIGHT CHANGE MEASUREMENTS

Weight change data in mg/cm^2 versus number of cycles for uncoated and coated 347H SS specimens subjected to oxidation at 800ºC for 50 cycles were plotted and shown in Fig.(5.3). It can be seen from the graph that both coated sample and bare sample followed parabolic behaviour. Parabolic rate constant Kp was also calculated for both the samples (bare as well as Ni25Cr). Values of K_p are shown in table. 5.1

5.1.1.3 SEM/EDS

Surface morphology of bare and coated samples after subjected to 50 cycles of oxidation at 800°C has been shown in fig ((5.5) and (5.6)). From figure 5.5 it can be seen that dense rhombohedral oxide layer was formed on the bare 347H SS sample. High Cr and oxygen content were shown by EDS thus it can be inferred that Cr oxide layer was formed on the surface of sample that was protecting the metal form further oxidation. Minor amount of molybdenum and

nickel were also found in the oxide layer. Mo and Ni were present in the substrate which diffuses towards the oxide when exposed at high temperature. Figure 5.6 shows the surface morphology of NiCr coated 347H SS. It can be clearly observed that dense oxide was formed on the surface of the coating. Figure 5.6(c) indicates that the oxide was present in the form of dense clusters. EDS analysis show that the oxide mainly consisting of nickel, chromium and oxygen. This may represents the formation of $NiCr_2O_4$ spinel and Cr_2O_3.

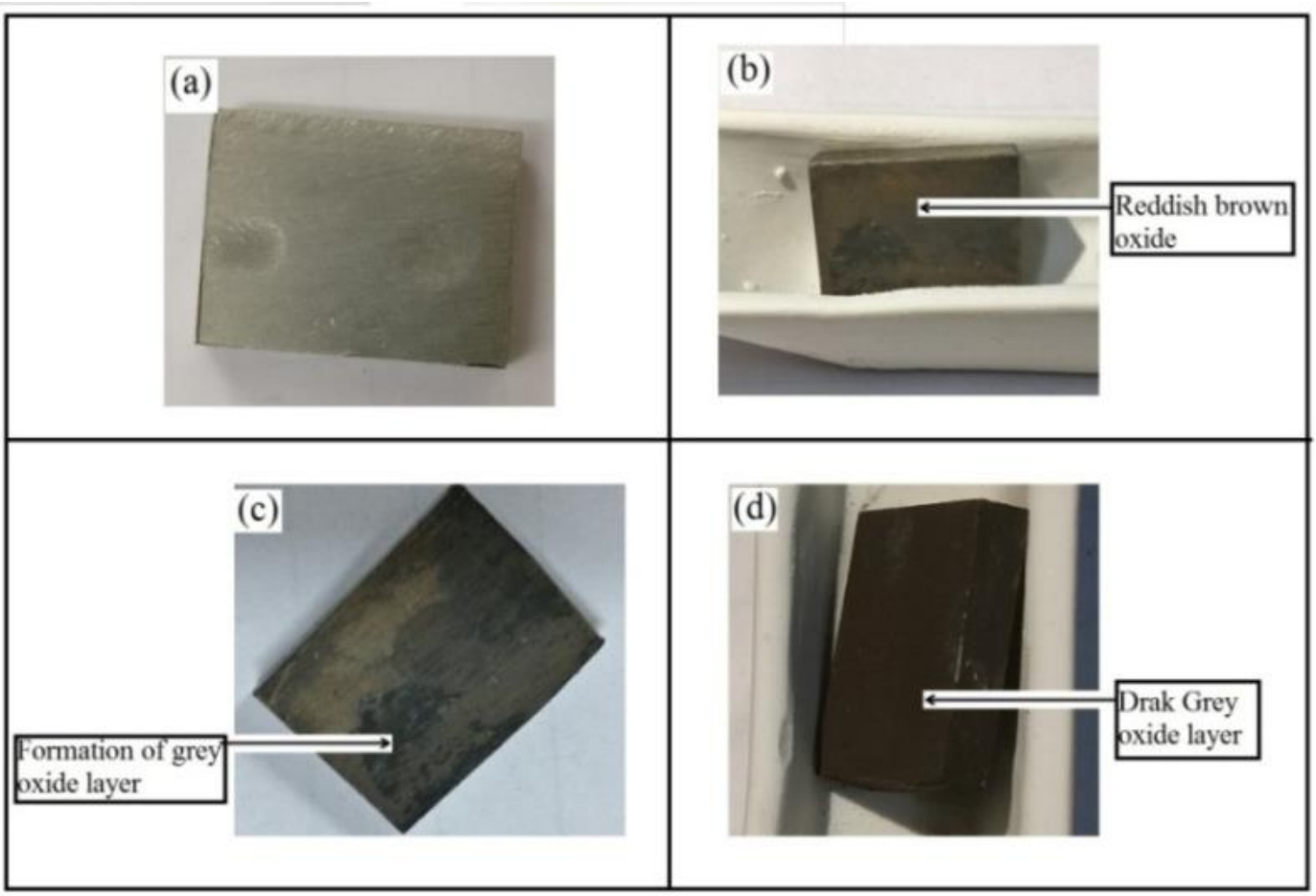

Fig 5.1: Visual macro-photos of (a) Polished Bare 347H SS and after subjected to oxidation in air at 800°C for (b) 1st cycle, (c) 15th cycle (d) 50th cycles.

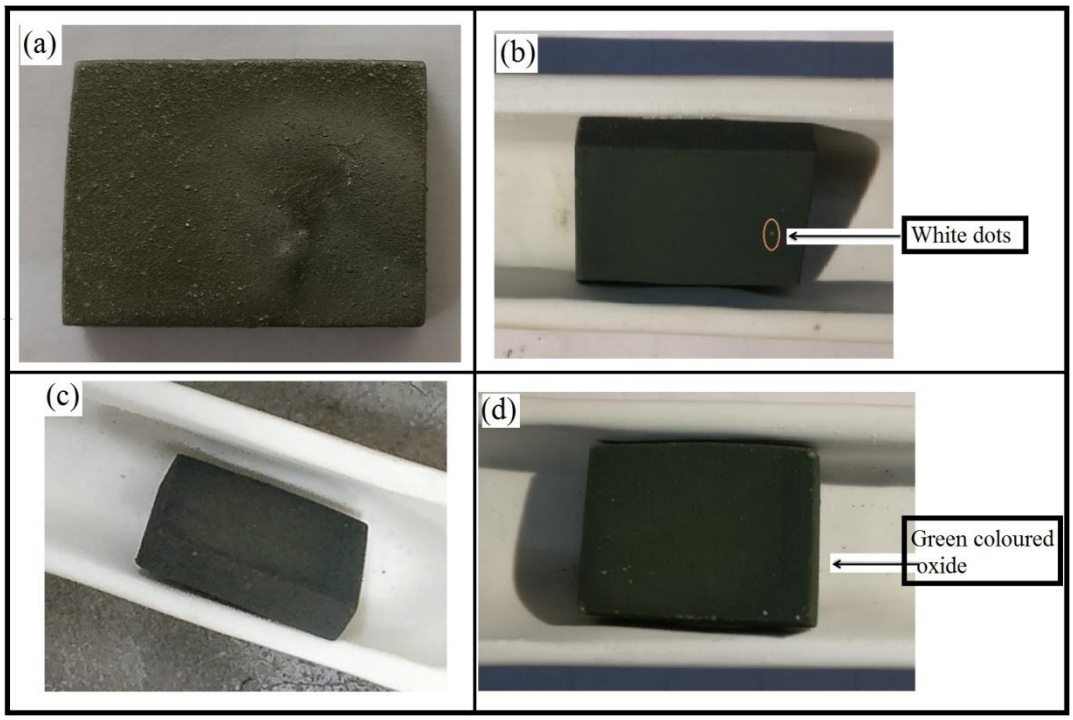

Fig 5.2: Visual macro photos of (a) NiCr coated 347H SS and after subjected to oxidation in air at 800°C for (b) 1st cycle, (c) 15th cycle (d) 50th cycles.

Table 5.1: k_p values of bare 347H SS and Ni25Cr coated stainless steel

Substrate	Parabolic rate constant K_p ($10^{-8}g^2cm^{-4}s^{-1}$)
Bare 347SS	0.011
NiCr Coated 347SS	0.005

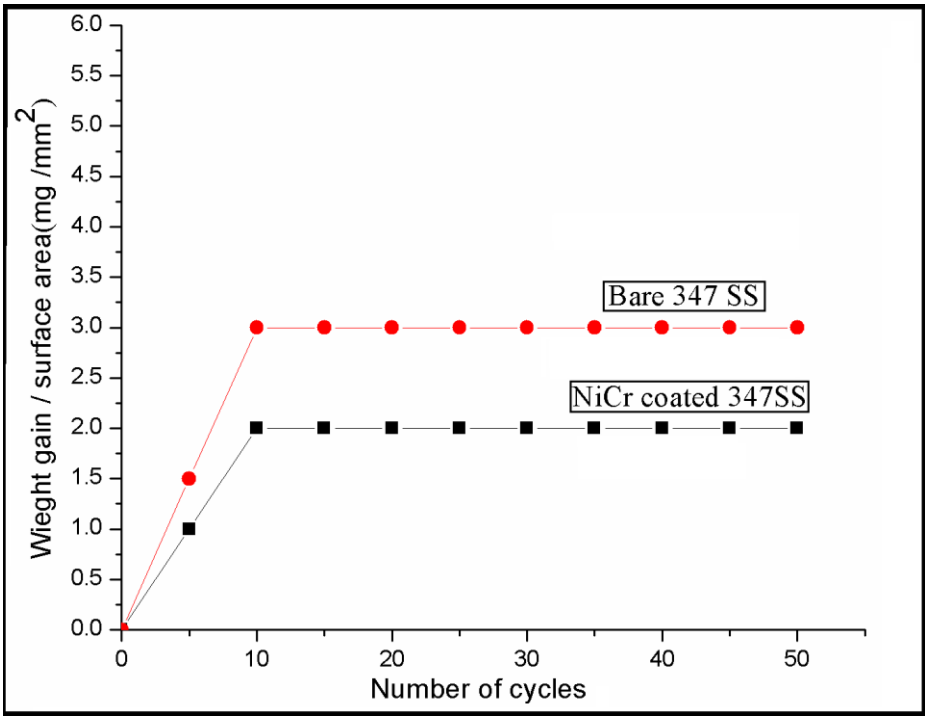

Fig 5.3: Weight gain/area *vs.* number of cycles plot for bare 347H SS and coated 347H SS subjected to cyclic oxidation at 800°C for 50 cycles.

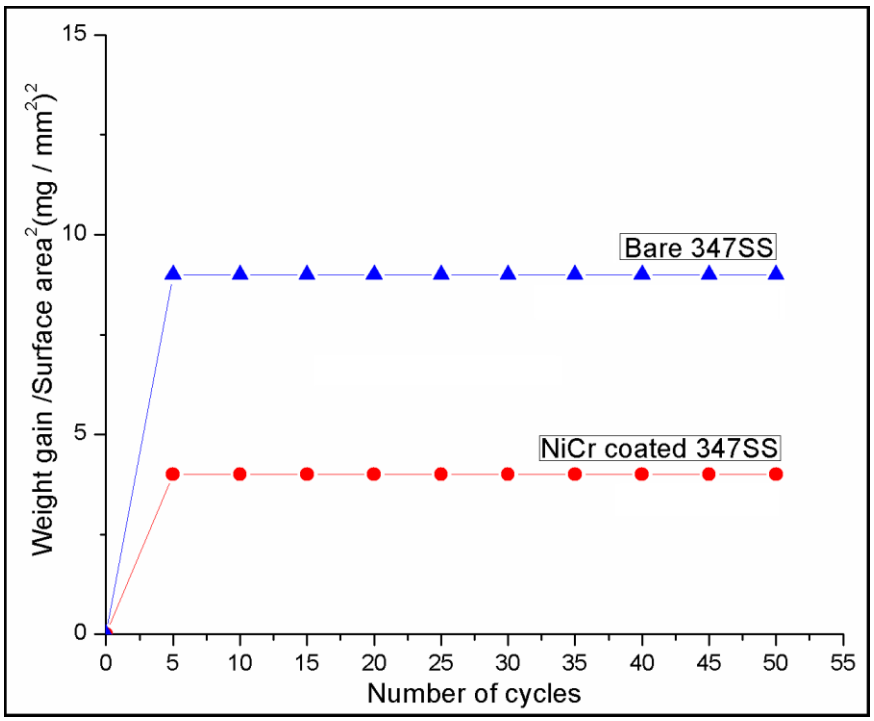

Fig 5.4: $(\text{Weight gain/area})^2$ *vs.* number of cycles plot for bare 347H SSand coated 347H SS subjected to cyclic oxidation at 800°C for 50 cycles.

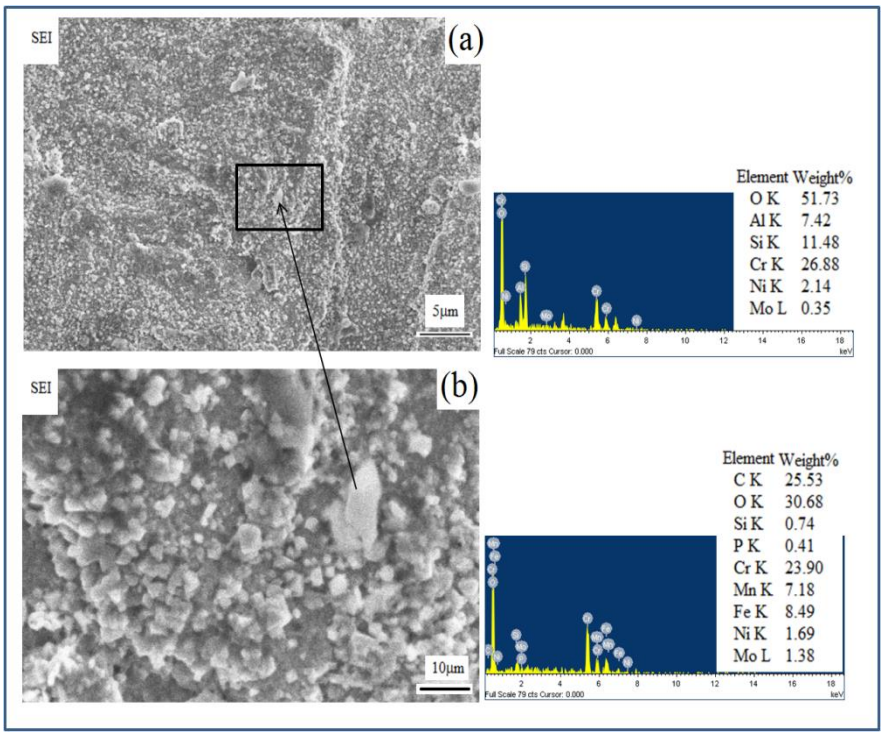

Fig 5.5: SEM/EDS analysis of oxidized bare 347H SS sample after 50 oxidation cycles at 800°C at a magnification of (a) 500X , (b) 2000X.

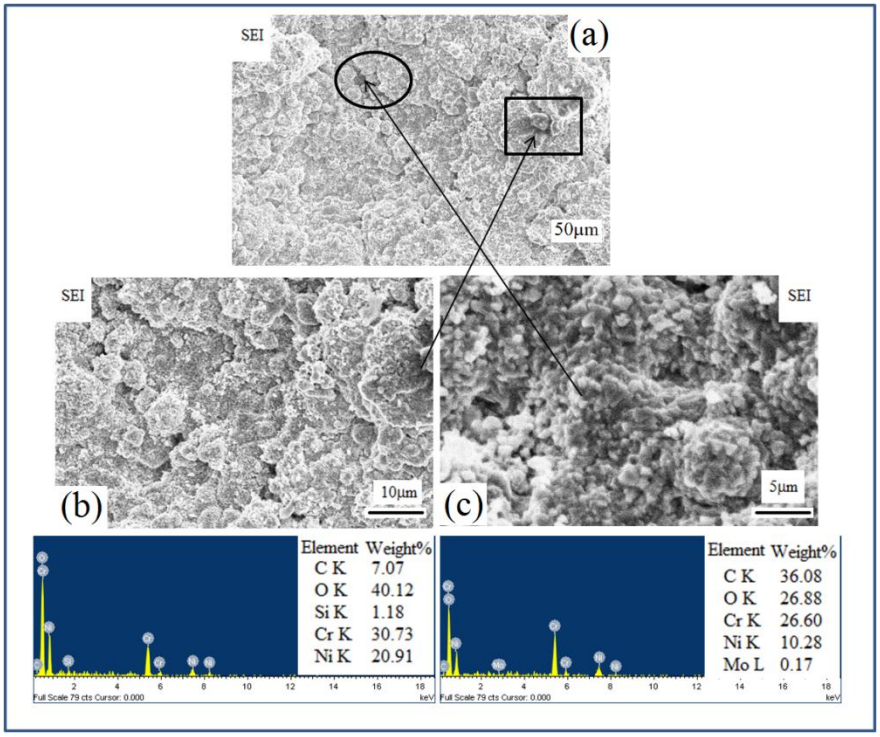

Fig 5.6: SEM/EDS analysis of oxidized NiCr coated 347H SS sample after 50 oxidation cycle at 800°C at a magnification of (a) 500X, (b) 1000X and (c) 2000X.

5.1.1.4 XRD

X-ray diffraction technique was used to identify the phases formed on the surface of corroded samples. For Bare 347H SS and coated 347H SS that have gone under oxidation test for 50 cycles, XRD analysis has been shown in figure (5.7). It can be observed that in both bare 347H SS steel and NiCr coated 347H steel, formation of major amount of Cr_2O_3 and $NiCr_2O_4$ occured. Cr_2O_3 was identified as the main phase.

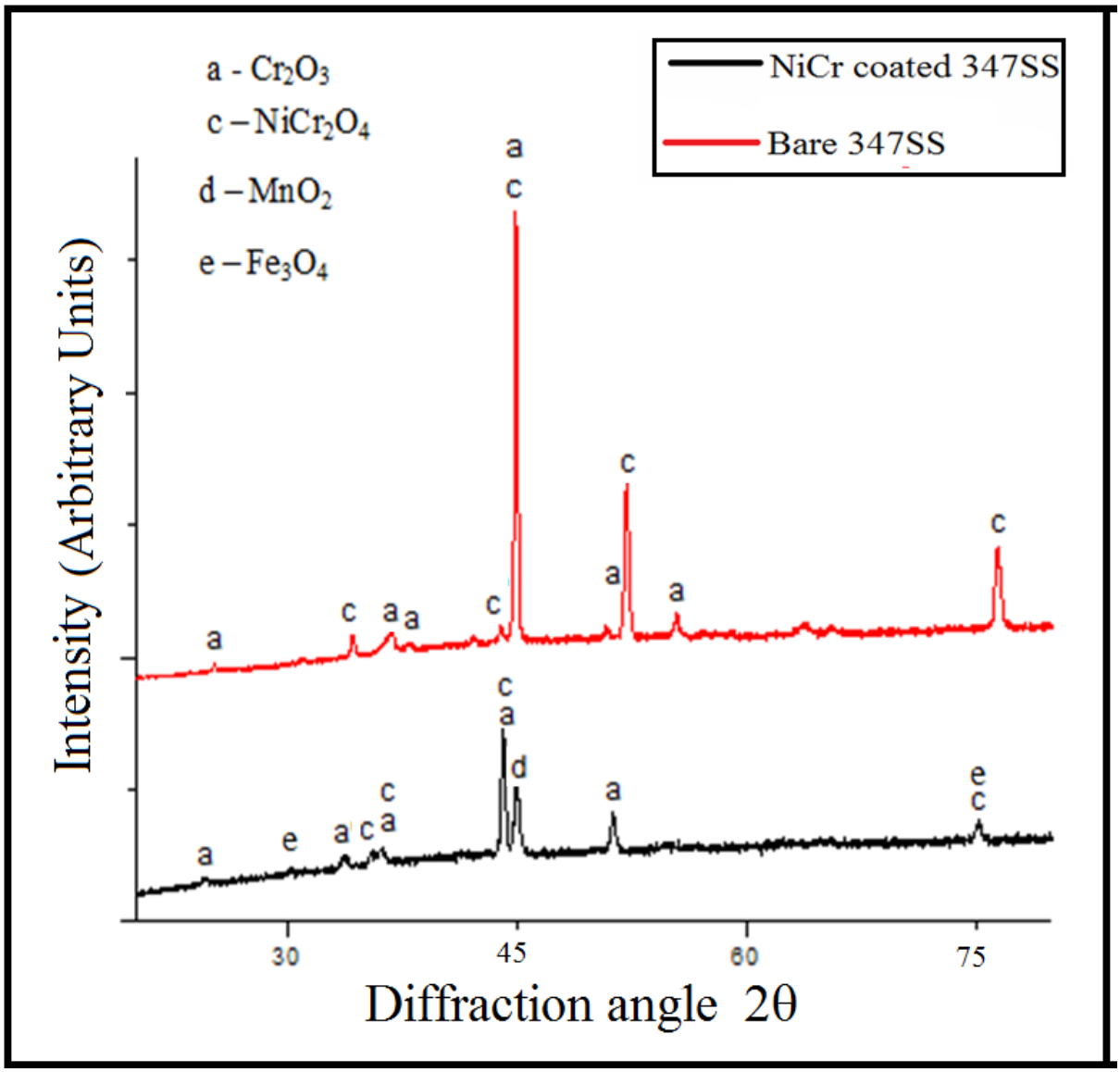

Fig 5.7: XRD analysis of bare 347H SS and NiCr coated 347H SS under oxidation for 50 cycles at 800ºC.

5.1.1.5 ELEMENTAL X-RAY MAPPING

X-ray mapping was done in order to find out the various elements present at the cross section of oxidized substrate. X-ray mapping was done across the cross section of the surfaces so as to indentify various elements present in the oxide scale, metal region and coated region. Both back scattered electron images and secondary electron images were taken about the cross section of specimens. Thickness of oxide scale was also measured from BSE image. It was found by BSE Image that the average thickness of oxide scale for bare 347H H stainless steel was 22.096μm. It can be clearly shown from fig (5.8) presence of various elements (O, Cr, Ni, Fe, Mn) in different regions (metal, oxide and Epoxy) of substrate. High presence of Cr, Ni, Fe and O can be seen in oxide region it can be due to formation of there oxides. Similarly the distributions of various elements inside the cross section of NiCr coated substrate showed are shown in fig (5.9).

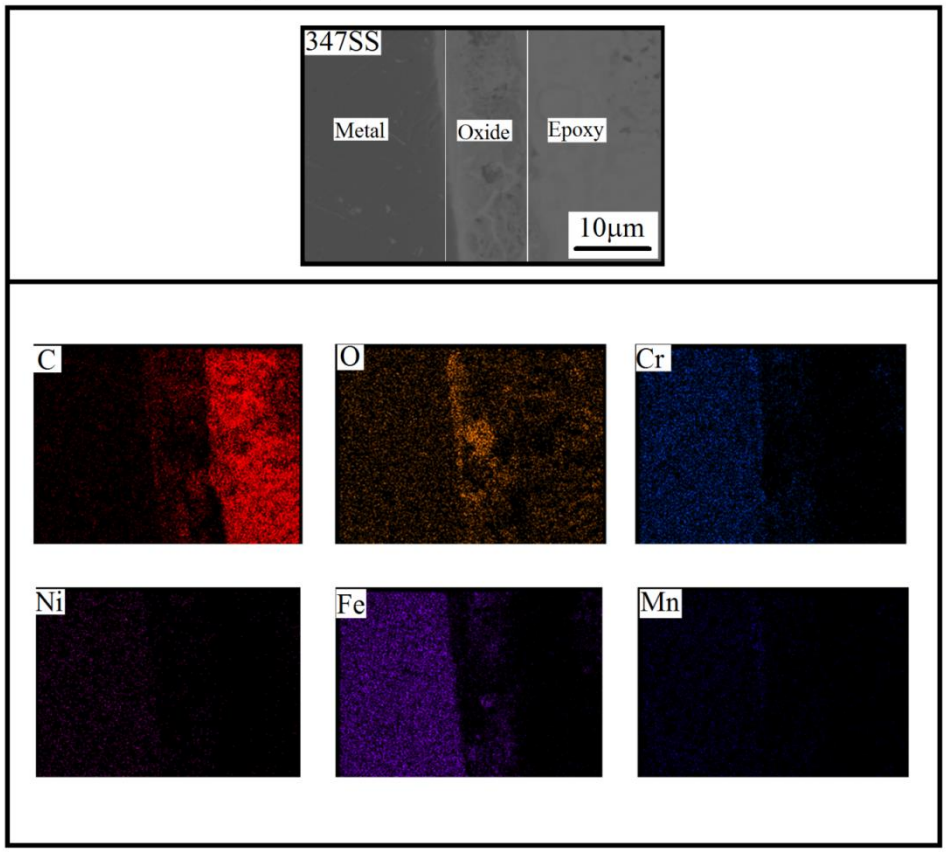

Fig 5.8: X-ray mapping analysis of bare 347H stainless steel after 50 cycles of oxidation in air at 800ºC .

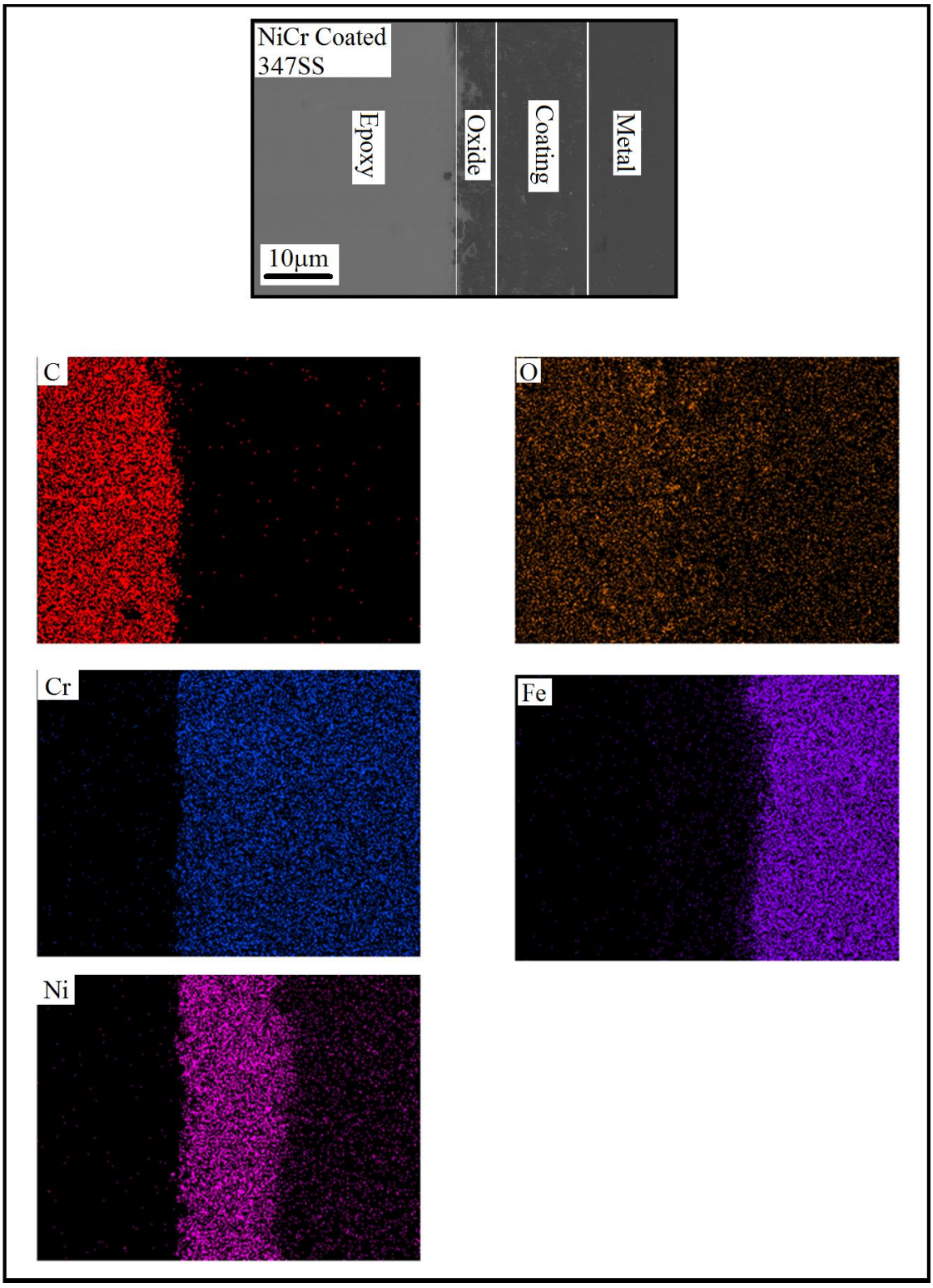

Fig 5.9: X-ray mapping analysis of 75Ni25Cr coated 347H SS after 50 cycles of oxidation in air at 800ºC.

5.2 DISCUSSION

From visual macrophotos it can be clearly observed that both bare and NiCr coated 347H steel showed good corrosion resistance after oxidation in air at 800ºC. No spallation or sputtering was observed throughout the 50th cycle. Occurrence of reddish orange oxide just after the 1st cycle may be due to rapid formation of iron oxide (Fe_3O_4) (Pettersson et al. 2005). Weight gain analysis depicted that both the samples have good oxidation resistance which may be due to presence of Cr and Ni which forms the protective oxide when combines with oxygen (Gupta et al. 2012). Weight gain graph of bare 347H stainless steel showed a little weight gain during initial cycles. Increase in weight gain during initial cycles may be due to initial formation of oxide scale. Rhombohedral oxide morphology was observed in SEM analysis and EDS analysis revealed presence of Cr and O. While in case of NiCr coated sample, dense and compact oxide was observed. It was found from EDS analysis that chromium, nickel and oxygen were the main elements present on the layer. Presence of Cr may be attributed to the formation of chromium oxide (protective oxide layer). In the literature it was reported by (Pang et al. 2007) (Mougin et al. 2001) that Cr_2O_3 scale has rhombohedral structure. Thus it can be inferred that the Cr_2O_3 oxide layer was formed in case of both the specimens. XRD analysis also revealed that the both specimens consist of Cr_2O_3 as protective oxide layer. Moreover X-ray mapping for coated steel also depicted nickel rich splats. Chromium and oxygen were present along the splats throughout the coating thereby signifying the formation of chromium oxide along the splat boundaries. Uniform continuous chromium oxide layer was found on the top of the surface of the coating and also along the coating substrate interface. Nickel remains unoxidised whereas chromium forms chromium oxide within the coating.

5.3 CONCLUSIONS

1. Ni25Cr coating was successfully deposited on 347H stainless steel using detonation gun technique.
2. Bare 347H stainless steel underwent very minor spallation only after 1st cycle of oxidation. Ni25Cr coating remains intact throughout the 50 cycle of oxidation
3. Both bare and Ni25Cr coated 347H stainless steel follows parabolic rate law after subjected to cyclic oxidation for 50 cycle at 800°C.

4. Cr oxide is mainly responsible for providing protection in case of bare 347H SS whereas in case of coated 347H stainless steel, $NiCr_2O_4$ and Cr_2O_3 oxides are providing protection against oxidation degradation till 50^{th} cycle.
5. Dense rhombhedral grey coloured oxide layer was formed on the bare 347H steel sample. SEM/EDS analysis showed Cr, O and Ni where present in major quantities.XRD analysis revealed Cr_2O_3 as major peak present in substrate.
6. Dense globular structured oxide layer is formed and EDS analysis detects presence of chromium, nickel, carbon, oxygen and molybdenum. XRD analysis determined presence of Cr_2O_3 and $NiCr_2O_4$ which may have protected substrate from further oxidation.

CHAPTER 6

HOT CORROSION STUDIES IN SIMULATED BOILER ENVIRONMENT

6.1 RESULTS

6.1.1 VISUAL ANALYSIS

The substrates during High temperature corrosion study showed change in color due to oxide scale formation on the top of the surface of specimens at a temperature of 800ºC. Macro-photos of bare 347H steel and 75Ni25Cr coated 347H steel after 1st cycle, 15th cycle and 50th cycle of hot corrosion test at 800°C has been shown in fig 6.1 and 6.2 respectively. Orange colored oxide scale was formed of bare 347H stainless steel after the completion of 1st cycle. After 15th cycle noticeable spallation was observed and the color of oxide layer changed to light blue with light orange patches on it. Subsequently after 50th cycle high amount of sputtering of bare 347H SS was observed. In case of 75Ni25Cr coated sample showed better resistance to corrosion as there was negligible amount of spallation. From fig (6.2) it can be clearly seen that color of sample changed to greenish blue after 1st cycle. No color change after 1st cycle was observed.

6.1.2 WEIGHT CHANGE ANALYSIS

The weight change values were measured at the end of each cycle to know the corrosion kinetics. Weight change data in mg/cm^2 versus number of cycles for uncoated and coated 347H SS specimens subjected to oxidation at 800ºC for 50 cycles were plotted and shown in Fig ((6.3) and (6.4)). It can be seen from the graph that both coated sample and bare sample followed parabolic behavior. Parabolic rate constant K_p was also calculated for both the samples (bare as well as Ni25Cr). Values of K_p are shown in table. 6.1

6.1.3 SEM/EDS

SEM is a technique that is used to examine the Surface morphology of the scale formed on the surface of the substrate at higher magnification. While as EDS technique detects approximate

percentage of each element that is present at the surface of substrate. Oxide scale formed on the surface of bare 347H stainless steel and 75Ni25Cr coated 347H stainless steel after cyclic oxidation has been shown in Fig. ((6.5) and (6.6)).Irregular structure and porous oxide scale was found in case of bare 347H SS fig (6.5) and in case of NiCr coated 347H SS, platelets like structure was formed fig (6.6). The presence of chromium and oxygen on the surface of both the specimens in major quantity was found by EDS analysis, this might be due to the presence of high quantity of Cr_2O_3. The presence of Cr_2O_3 was also detected by XRD analysis which proves its occurrence

Table 6.1: k_p values of bare 347H SS and Ni25Cr coated stainless steel

Substrate	Parabolic rate constant K_p ($10^{-8}g^2cm^{-4}s^{-1}$)
Bare 347SS	2
NiCr Coated 347SS	0.1

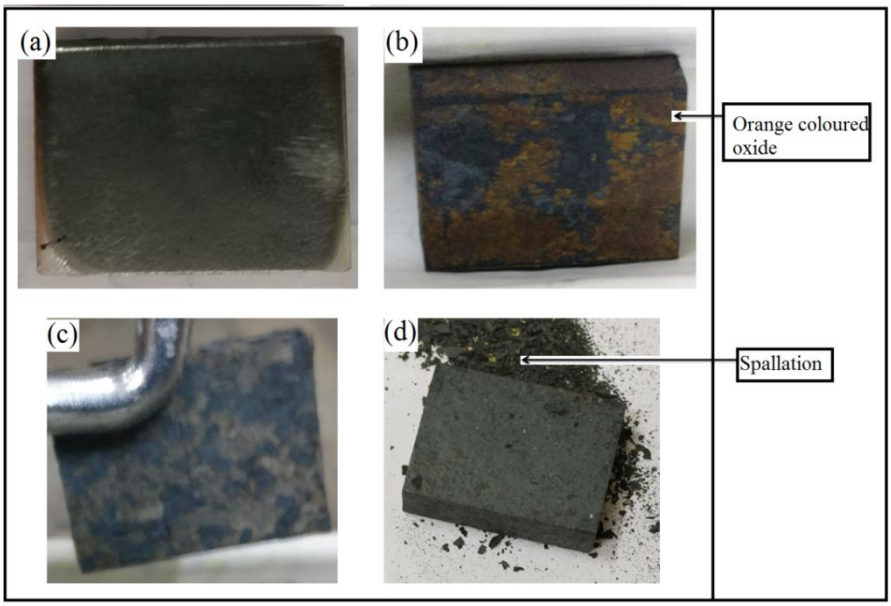

Fig 6.1: Visual macro-photos of (a) Polished Bare 347H SS and after subjected to corrosion test in salt environment (40%Na_2SO_4, 10%NaCl, 40%K_2SO_4, 10%KCl) at 800°C for (b) 1st cycle, (c) 15th cycle (d) 50th cycles.

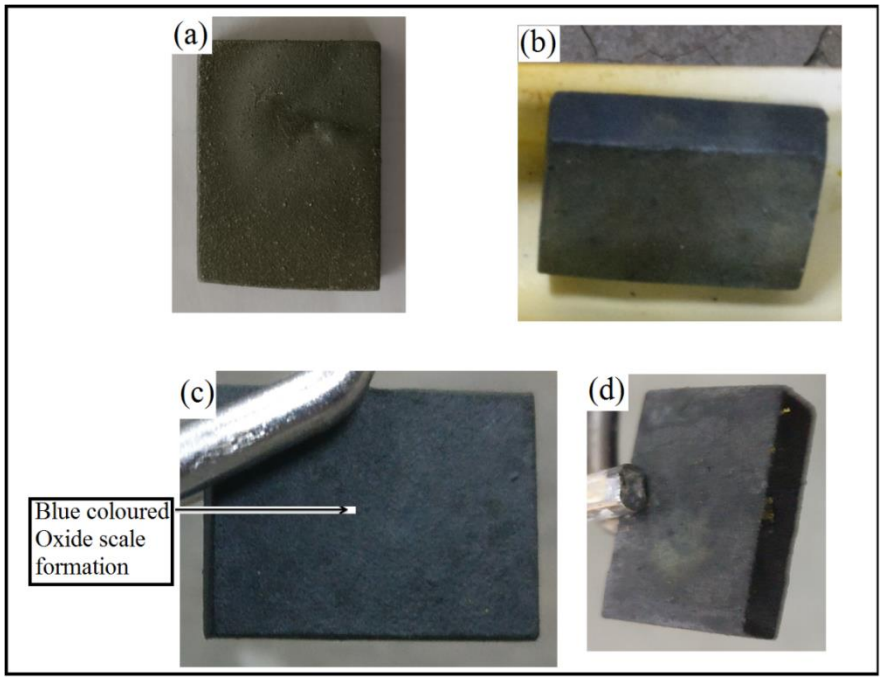

Fig 6.2: Visual macro-photos of (a) NiCr coated 347H SS and after subjected to corrosion test in salt environment (40%Na_2SO_4, 10%NaCl, 40%K_2SO_4, 10%KCl) at 800°C for (b) 1st cycle, (c) 15th cycle (d) 50th cycles.

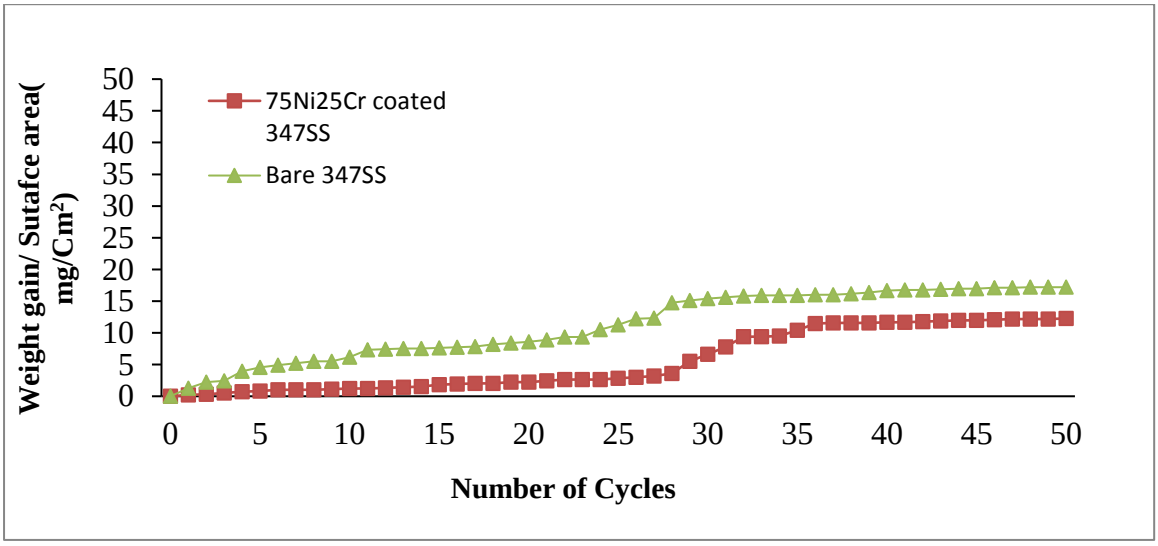

Fig 6.3: Weight gain/area *vs* number of cycles plot for bare 347H SS and NiCr coated 347H SS subjected to cyclic oxidation

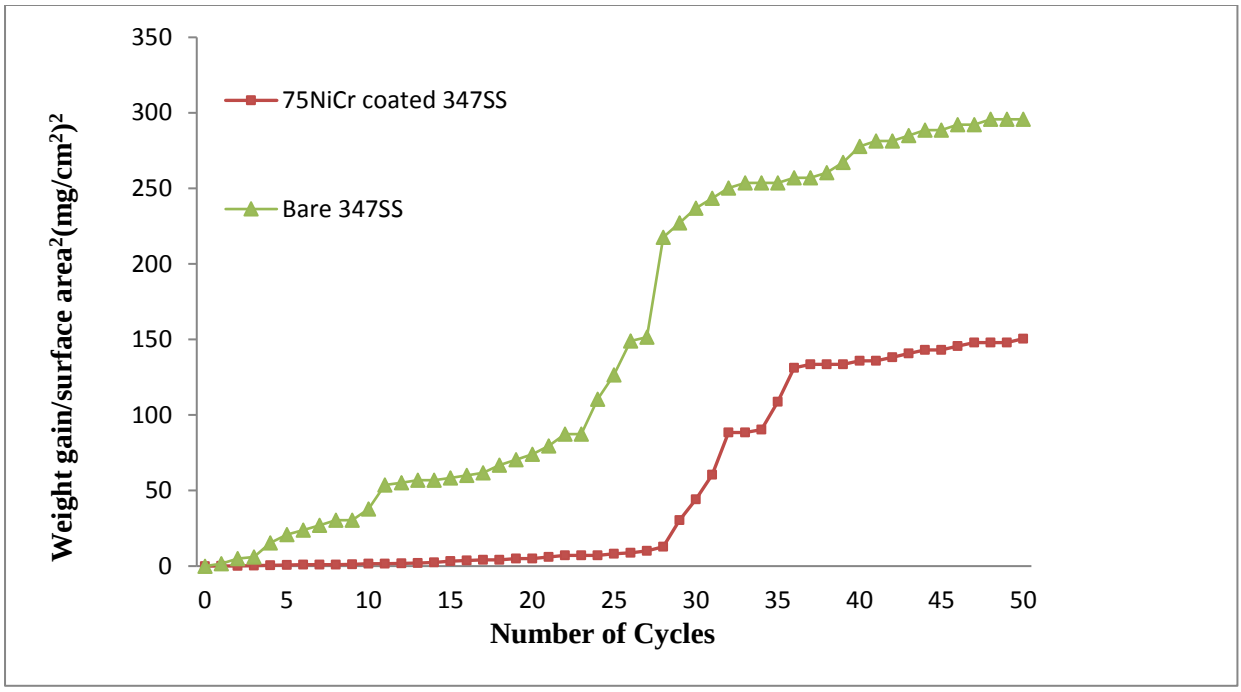

Fig 6.4: (Weight gain/area)^2 *vs* number of cycles plot for bare 347H SS and coated 347H SS subjected to cyclic oxidation.

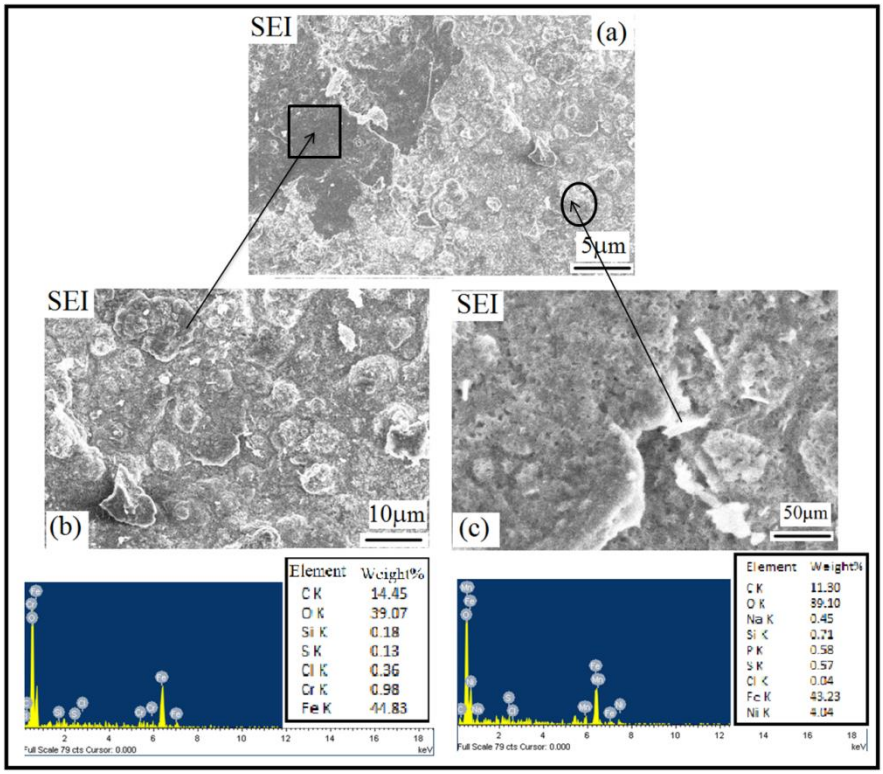

Fig 6.5: SEM/EDS analysis of hot corroded bare 347H SS after 50 cycles at 800ºC.

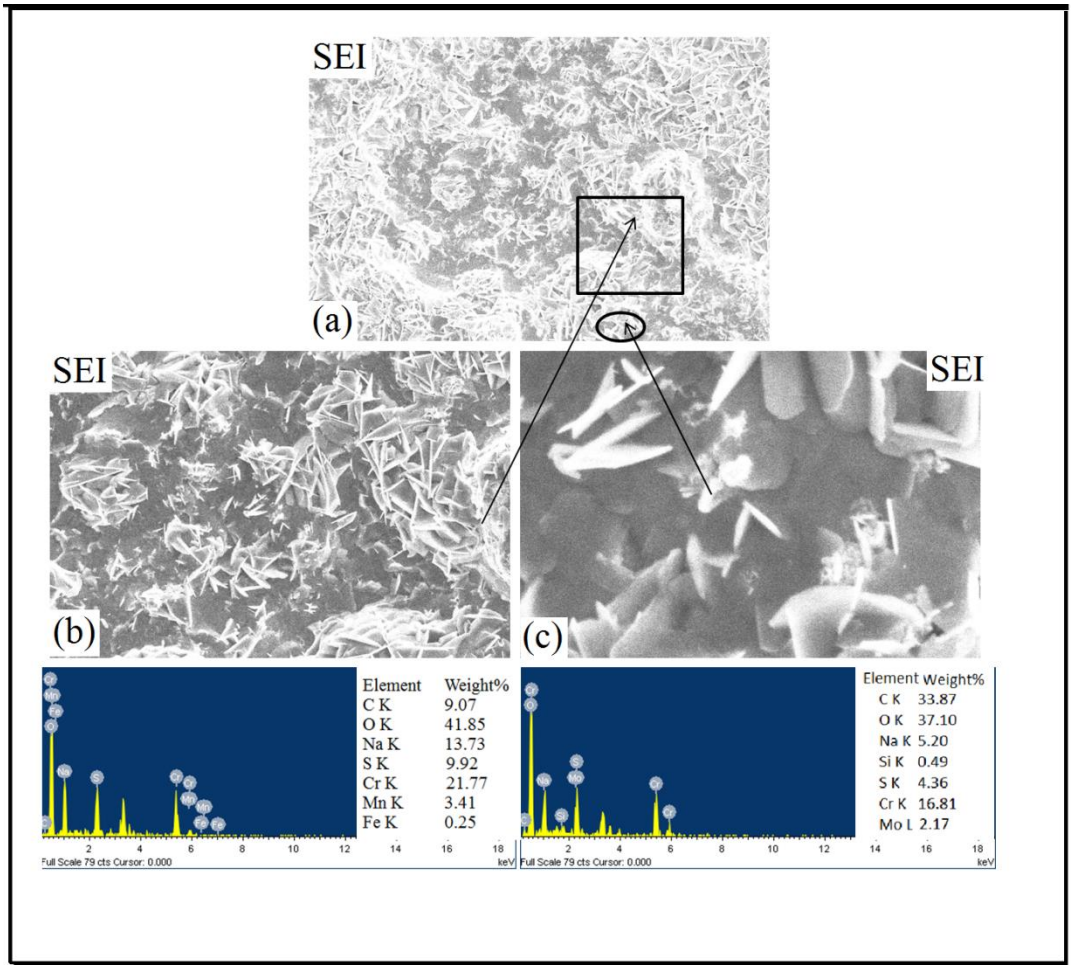

Fig 6.6: SEM/EDS analysis of hot corroded NiCr coated 347H SS after 50 cycles at 800ºC.

6.1.4 XRD

XRD diffractograms for coated and uncoated 347H stainless steel subjected to high temperature corrosion in (40%Na_2SO_4, 10%NaCl, 40%K_2SO_4, 10%KCl) environment at 800˚C for 50 cycles are depicted in figure (6.7).To identify various phases present in the bare and coated 347H SS which have been run under hot corrosion test, XRD analysis was done. XRD of bare sample shows the existence of corrosion protective oxides of, Cr_2O_3, $NiCr_2O_4$, NiO, K_2CrO_4 etc. Presence of non-protective oxides i.e Fe_2O_3 was also found in bare 347H SS sample. On the other hand major peaks on coated sample were those that help in reducing rate of corrosion like Cr_2O_3, $NiCr_2O_4$, NiO, K_2CrO_4.

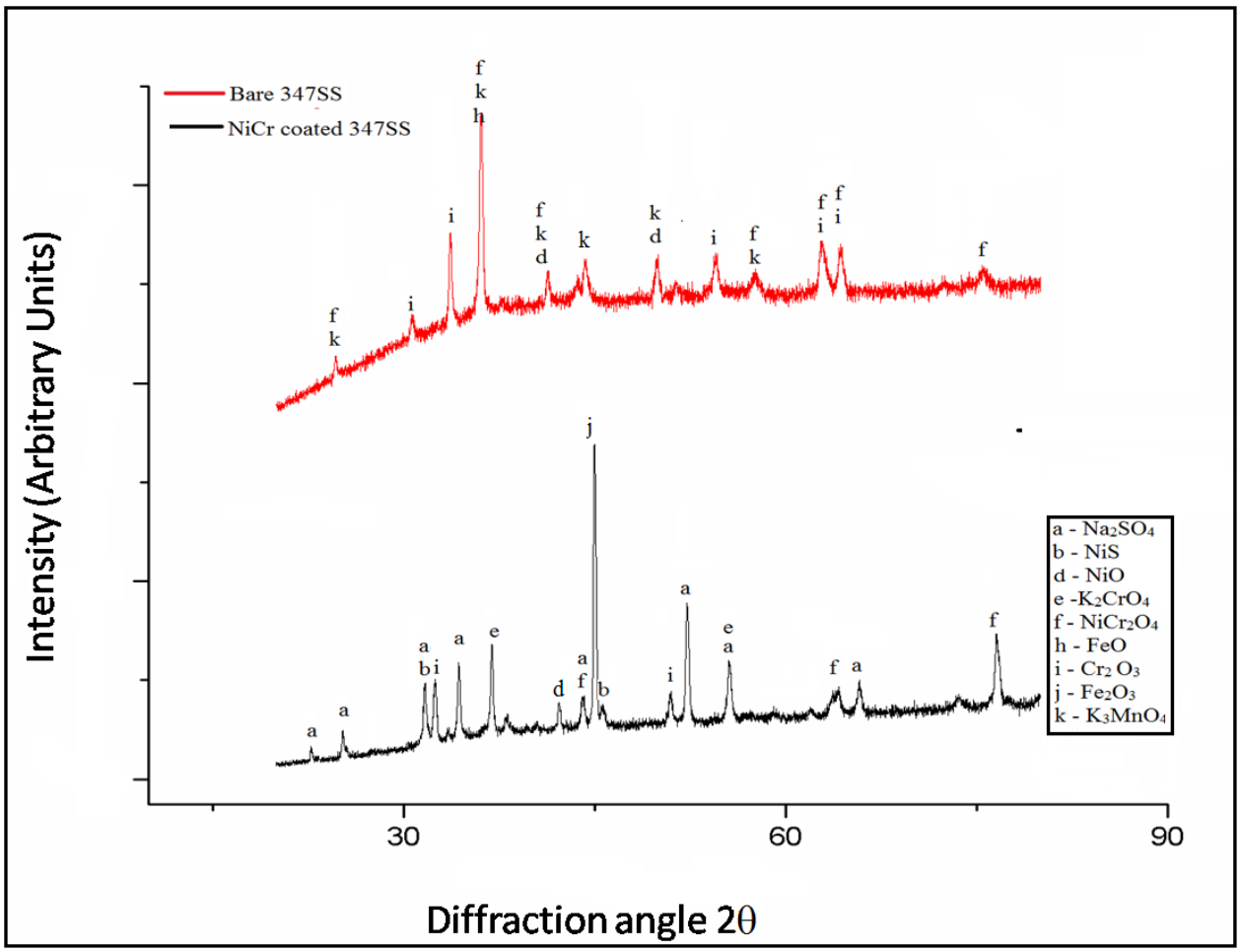

Fig 6.7: XRD analysis of bare 347H SS and NiCr coated 347H SS under high temperature corrosion for 50 cycles at 800ºC.

6.1.5 ELEMENTAL X-RAY MAPPING

The oxide layer of bare 347H SS (figure 6.8) under molten salt (40%Na_2SO_4, 10%NaCl, 40%K_2SO_4, 10%KCl) reveals that the scale is consisting of Cr, O, Mn, Fe elements. Whereas, in case of NiCr coated 347H SS steel (figure 6.9) showed the presence of chromium and oxygen throughout the oxide layer. It can be clearly understood form XRD analysis and X-ray mapping that the presence of Cr and Ni are forming protective Cr_2O_3 and $NiCr_2O_4$ oxide layer. High content of Cr presence in Coating regions depicts forming of Cr_2O_3 oxide layer that is protecting metal form corrosion.

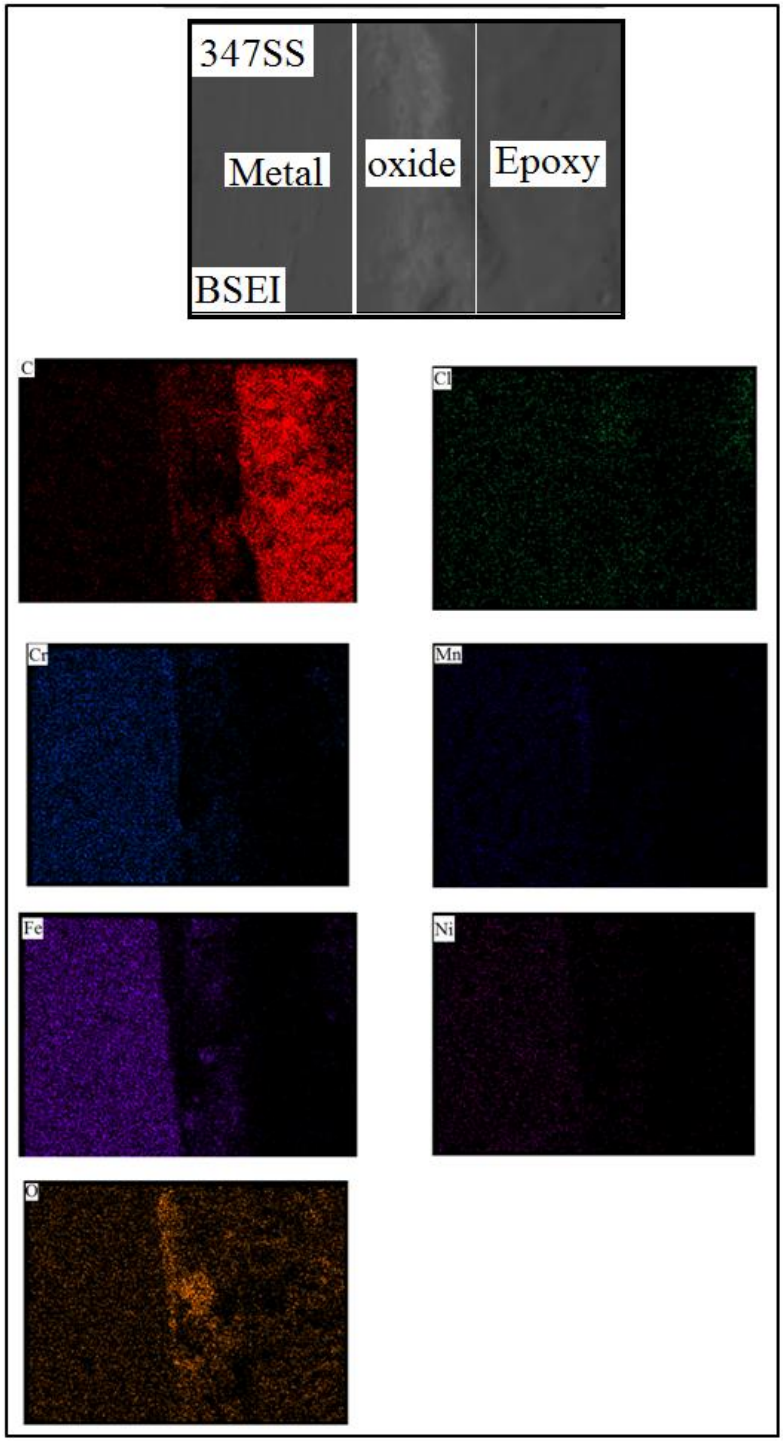

Fig 6.8: X-ray mapping of corroded 347H SS after 50 cycles under 40 %Na_2SO_4-40 %K_2SO_4-10 %NaCl-10 %KCl molten salt environment at 800°C.

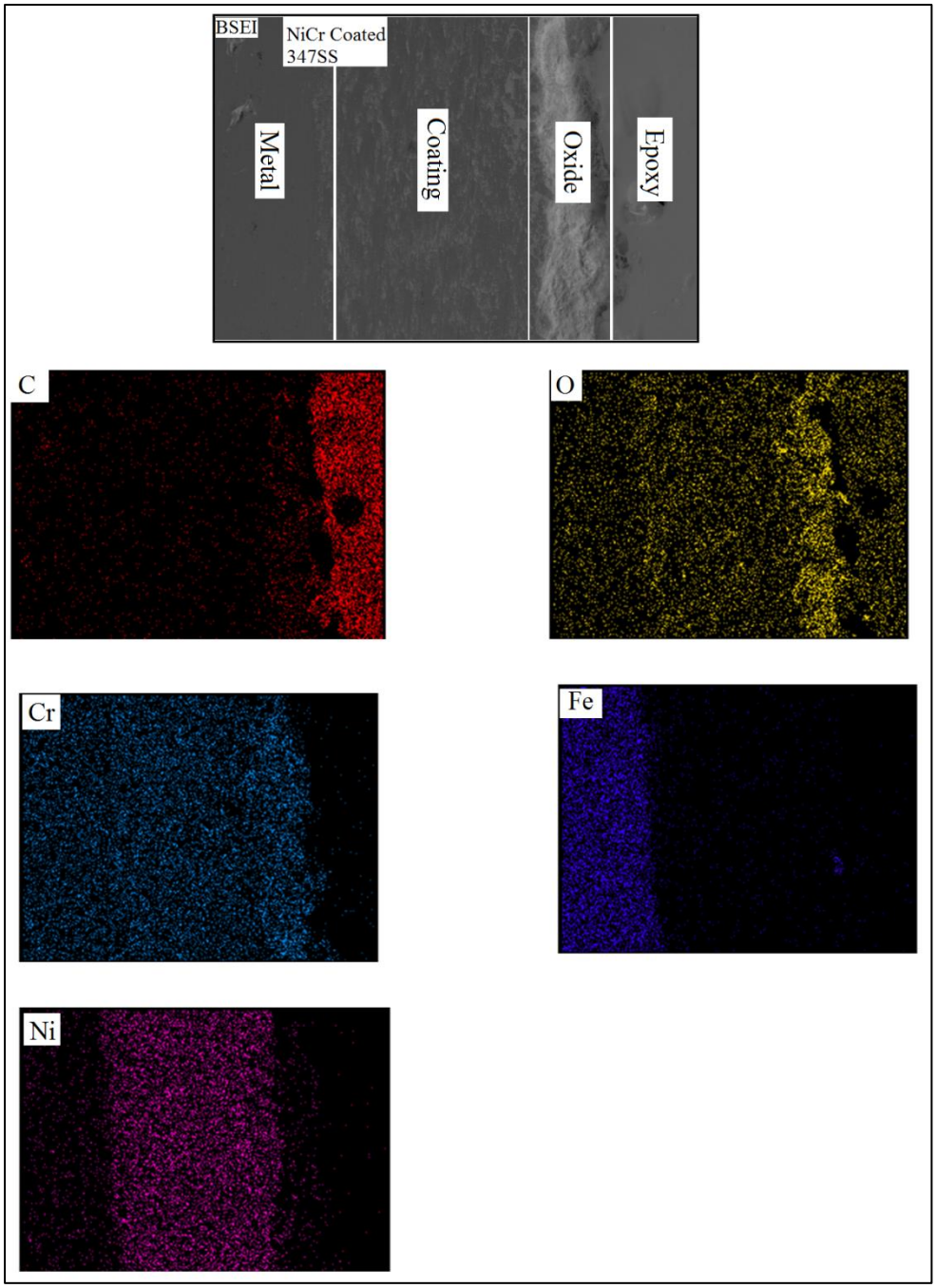

Fig 6.9: X-ray mapping of corroded 75Ni25Cr coated stainless steel after subjected to 50 cycles under 40 %Na_2SO_4-40 %K_2SO_4-10 %NaCl-10 %KCl molten salt environment at 800°C.

6.2 DISCUSSION

From visual analysis it can be seen that reddish orange colored oxide scale was formed in case of bare 347H SS. Presence of orange colored oxide scale can be due to formation of Fe_2O_3 (Pettersson et al. 2005).Formation of iron oxide might have occurred because of the existence of major amount of iron in the substrate which diffuses out from the metal and combines with the oxygen to form oxide. Another reason in this study which increases the possibility for the formation of iron oxide might be due to the presence of chlorine in the environment. The presence of Cl_2 in simulated salt solution reacts in Fe, forming volatile metal chlorides at the oxide/metal boundary, as shown in equation (6.1).

$$Fe(s)+Cl_2(g)\rightarrow FeCl_2(g) \quad \text{.....(6.1)}$$

These volatile metal chlorides then react with the oxide scale which results in formation of Fe_2O_3 and chlorine gas.

$$2FeCl_2(g)+(3/2)O_2(g)\rightarrow Fe_2O_3(s)+2Cl_2(g) \quad \text{.....(6.2)}$$

Similar results were found by (Grabke and Spiegel 1995). XRD shows (see Fig. 6.7), presence of potassium in the form of potassium chromate (K_2CrO_4) in both bare and coated 347H SS. Formation of this oxide can be due to this reaction shown in equation (6.2)

$$Cr_2O_3(s)+4KCl(s)+(5/2)O_2(g) \rightarrow 2K_2CrO_4(s)+2Cl_2(g) \quad \text{.....(6.3)}$$

As it can be seen from the composition of the base metal that higher amount of chromium is present in both coating and substrate. The chromium reacts with oxygen to form chromium oxide. The formation of Cr_2O_3 could be explained as Cr has good affinity towards O_2 and also posses least gibbs free energy than Ni or Fe. As it posses least gibbs free energy shown in fig (6.10), tendency of Cr to react with O is higher than other elements present like Fe and Ni. Hence when the metal is exposed at high temperature, chromium forms chromium oxide at much faster rate than iron. This oxide reacts with the potassium chloride to form potassium chromate. Moreover Cr_2O_3 oxide reduces effect of corrosion as it act as protective oxide layer (Gupta et al. 2012). It can be clearly indicated from XRD and EDS analysis that two main phases present in coated samples are Cr_2O_3 and $NiCr_2O_3$. Both these oxide are considered as corrosion protecting oxide layers.

From visual macrophoto (figure) of NiCr coated 347H SS, it can be seen that grrnish colour oxide was formed on the surface of coating. The formation of greenish layered oxide might be due to formation of NiO oxide (Mudgal et al. 2012).Weight gain analysis showed that

NiCr coated samples provided better protection towards corrosion than Bare 347H SS sample as K_p value of coated sample was far less than latter one .

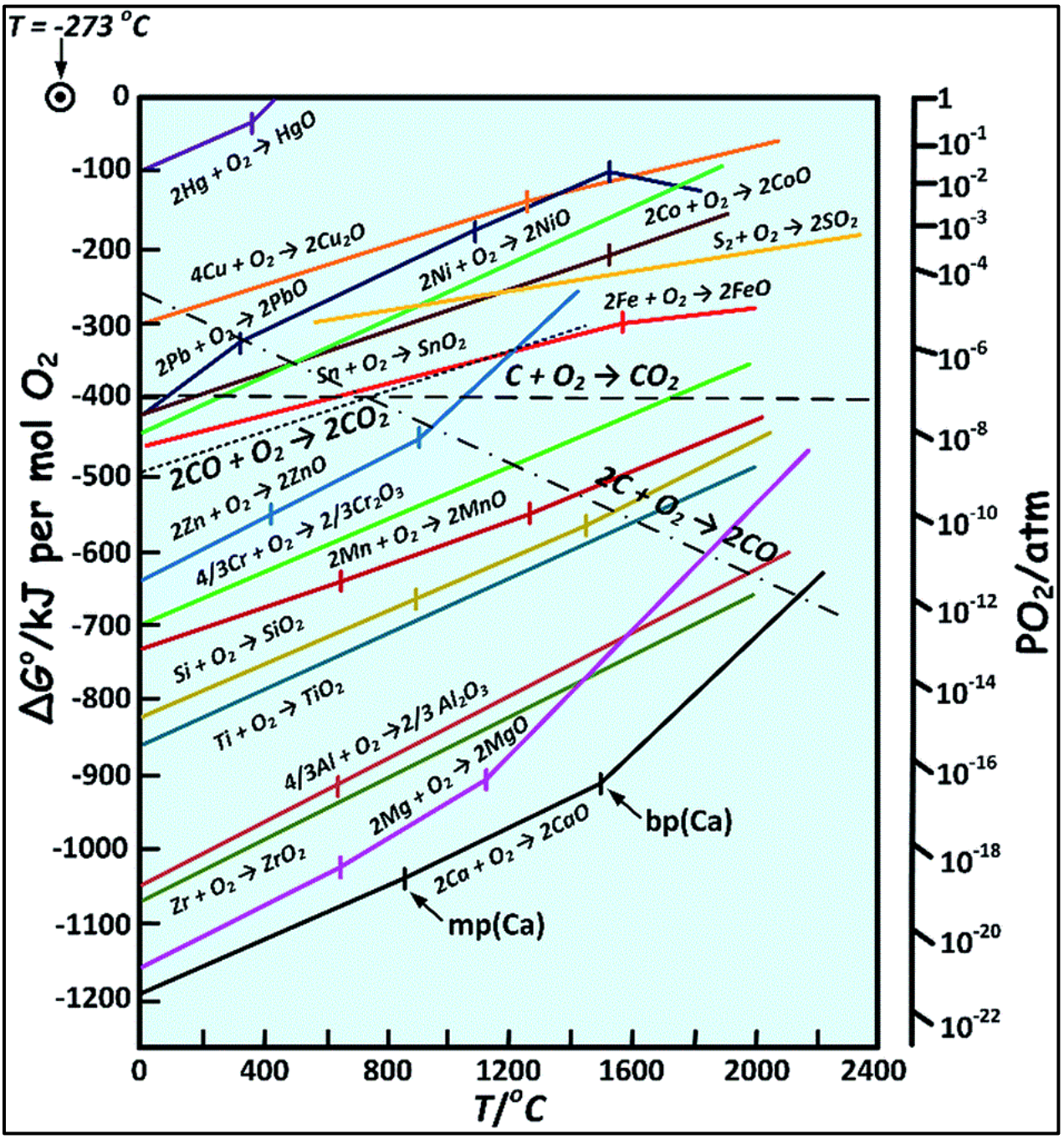

Fig 6.10: Ellingham diagram (Pettersson 2005).

6.3 CONCLUSION

1. D-gun spraying process has been successfully used to deposit 75N25iCr, coatings on 347H stainless steel specimens.
2. Based on overall weight gain after 50 cycles in simulated molten salt environment at 800°C for NiCr coated sample provided better protection than bare stainless steel sample.
3. Formation of Cr_2O_3 and $NiCr_2O_4$ oxides are mainly responsible for the better corrosion protection for NiCr coated substrate. Although Cr_2O_3 oxide layer was also found in XRD analysis of bare sample but it also revealed formation of Fe_3O_2 non protective oxide which may be the main cause for excessive sputtering of bare specimen.
4. During early few cycles, higher weight gain of samples were experienced in the present study in the given environments for both the samples. Nevertheless after formation of oxide scale around the specimens the rate of weight gain decreased.
5. Porous irregular shaped oxide layer was formed on the bare 347H SS sample. SEM/EDS analysis showed presence Fe, O and Ni where present in major quantities.XRD analysis revealed Fe_2O_3 as major peaks present in substrate which explains the reason for excessive spallation.
6. Dense platelet structured oxide layer is formed in case of NiCr coated sample and EDS analysis detects presence of chromium, oxygen in major quantity. XRD analysis determined presence of Cr_2O_3 and $NiCr_2O_4$ which may have protected substrate from earlier degradation as both these oxide layer have good affinity towards corrosion.

CHAPTER 7

HOT CORROSION STUDIES IN ACTUAL BOILER ENVIRONMENT

7.1RESULTS

7.1.1VISUAL ANALYSIS

The substrates during high temperature corrosion study in actual boiler environment showed change in color due to oxide scale formation on the top of the surface of specimens at a temperature range of of 700ºC-750ºC. Macro-photos of bare 347H SS and 75Ni25Cr coated 347H SS before and after subjected to high temperature corrosion in actual boiler environment conditions at a temperature range of 700°C-750ºC has been shown in fig 7.1 and 7.2 respectively. Dark grey colored oxide scale was formed of bare 347H stainless steel after the completion of 150 hours in boiler. On the other hand greenish oxide layer was formed on the surface of NiCr coated sample. It can be cleared seen form fig((7.1) and (7.2)) that large amount of metal loss could be seen in case of bare 347H SS. However NiCr coating provided better protection to substarte in harsh boiler environment. Thus less amount of metal loss was observed for NiCr coated samples.

7.1.2SEM/EDS

The SEM/EDS micrograph of bare and NiCr coated samples after subjected to 150 hours in actual boiler is shown in fig ((7.3) and (7.4)). SEM image for bare sample showed the formation of large granular iron oxides. EDS confirmed the elements present were mainly Fe and O only. Large cracks were observed which is due to the iron oxide scale which has low thermal coefficient of expansion. While cyclic heating the cracks appeared on the oxide scale. Also it can be seen that the oxide layer formed was of porous nature which was unable to stop the diffusion of the cations and anions which further increases the oxidation of the specimen. SEM graphs of NiCr coated 347H SS showed irregular microstructure which obviously signifies the formation

of the chromium oxide after the 150 hours in boiler. EDS showed the presence of O and Cr elements in major quantity along with Ni, Si and Fe.

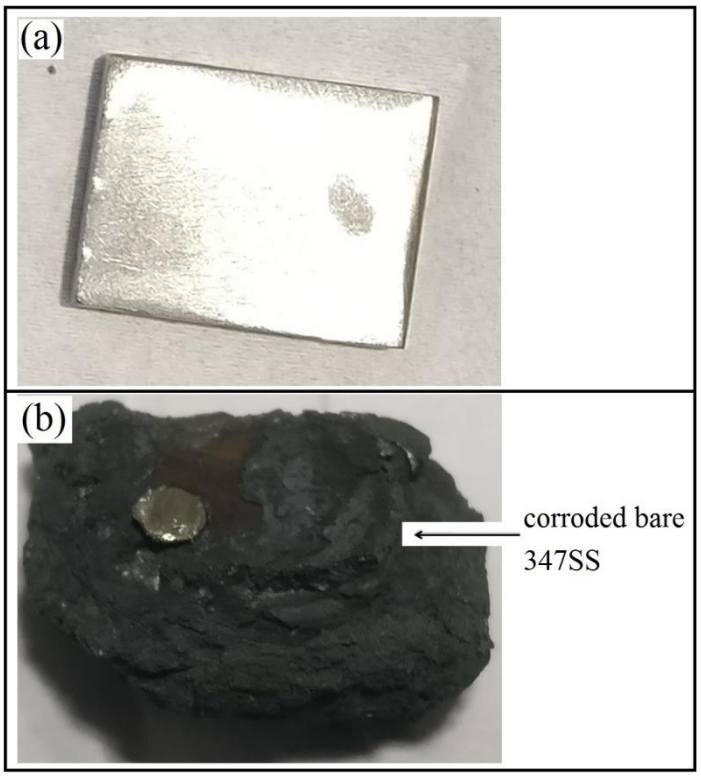

Fig 7.1: Visual macro-photos of Polished Bare 347H SS (a) before and (b) after subjected to corrosion test in actual boiler environment salt environment.

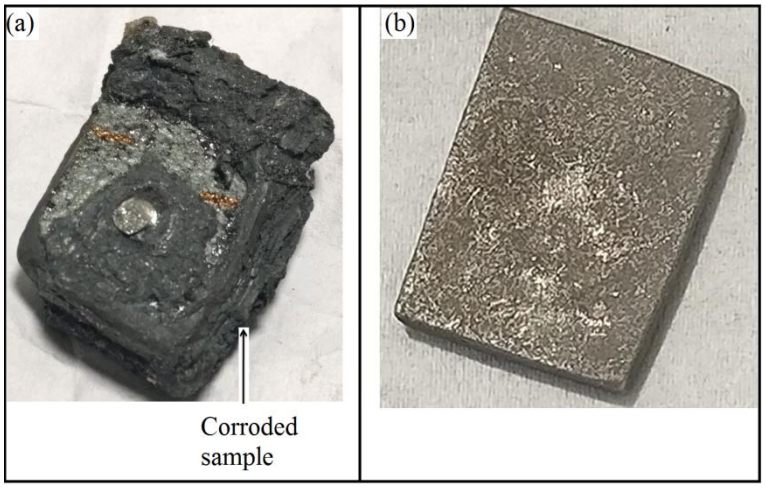

Fig 7.2: Visual macro-photos of NiCr coated 347H SS(a) after and (b) before subjected to corrosion test in actual boiler environment

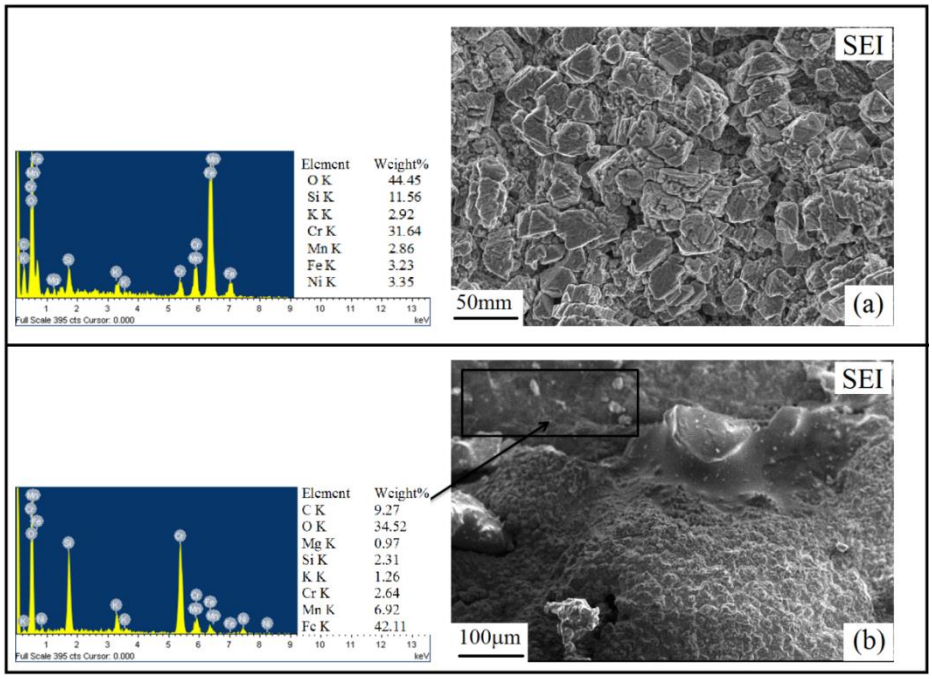

Fig 7.3: SEM/EDS analysis of hot corroded bare 347H SS in actual boiler environment for 150 hours at a magnification of (a) 2000X and (b) 500X

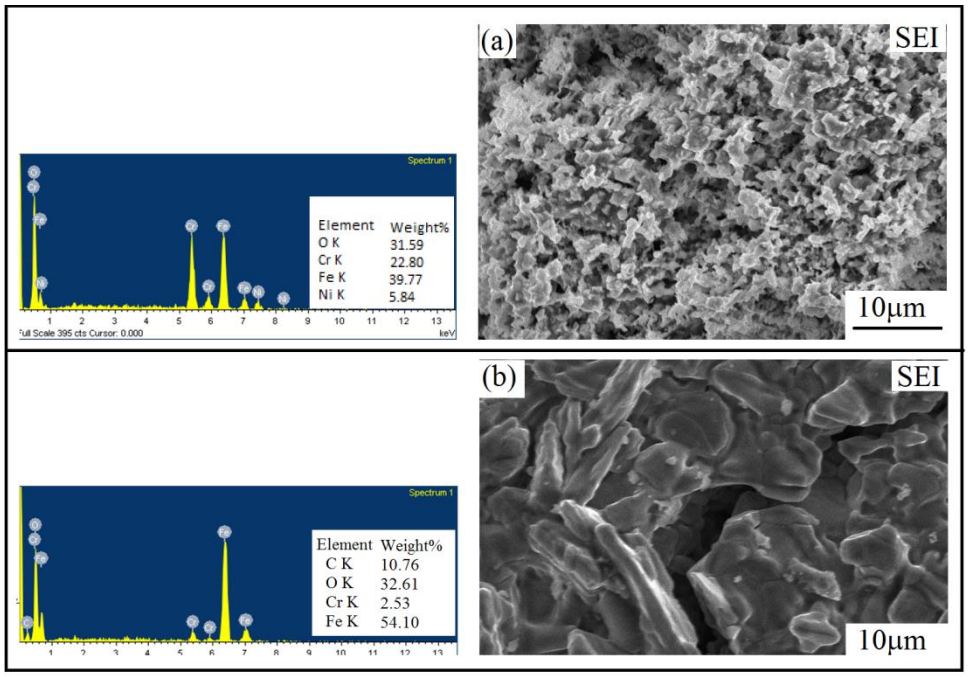

Fig 7.4: SEM/EDS analysis of hot corroded NiCr coated 347H SS at (a) 2000X and (b) 500X in actual boiler environment for 150 hours.

7.1.3 XRD

XRD analysis of bare 347H SS steel indicated the formation of Cr_2SiO_4, $NiCr_2O_4$, Fe_3O_4 and Cr_2SiO_4. Whereas NiCr coated 347H SS steel, depicted the formation of $NiCr_2O_4$, K_2CrO_4, Mg_2SiO_4, Fe_2O_3, Ni_2SO_4

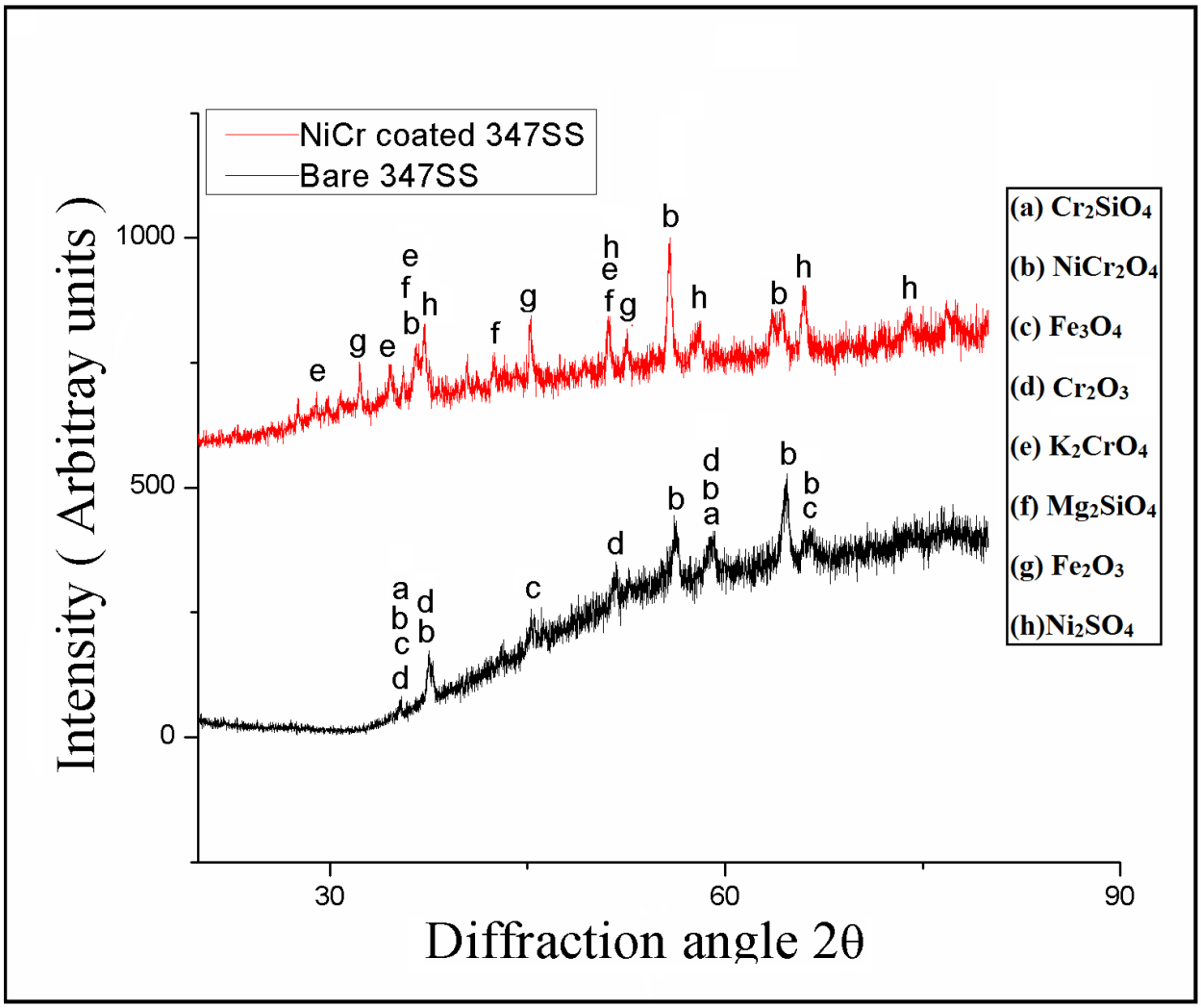

Fig 7.5: XRD analysis of bare 347H SS and NiCr coated 347H SS under high temperature corrosion in actual boiler environment for 150 hours.

7.1.4 ELEMENTAL LINE MAPPING

X-ray mapping technique was used to detect elements present in the oxide layer of substrates. The elements that were identified in case of bare 347H SS steel are O, Fe, Cr, C, Ni and Si. High presence of Cr and Fe can be seen in metal and oxide region from X-Ray mapping. Formation iron oxide leads to less protective performance of bare 347H SS steel. The XRD analysis also revalled the presence of two major phases in bare sample that were Fe_3O_4 (non protective oxide) and Cr_2O_3 (protective oxide) . However in case of 75Ni25Cr coating the elements that were present are C, Fe, Ni, Cr, Si and O.$NiCr_2O_4$ oxide was mainly responsible for providing protection to 75Ni25Cr coated steel sample.

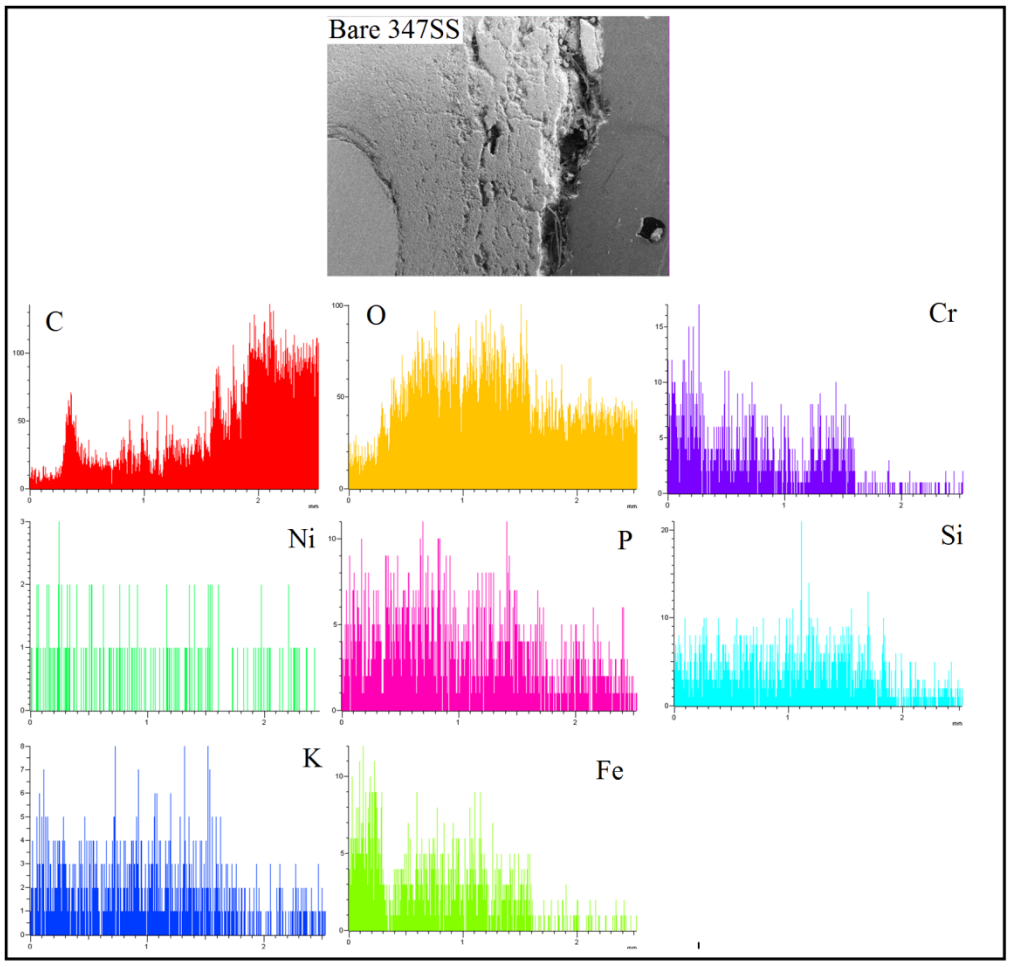

Figure 7.6: X-Ray mapping of bare 347H SS steel after exposed in husk fired boiler for 150 hours at a temperature range between 750±50ºC.

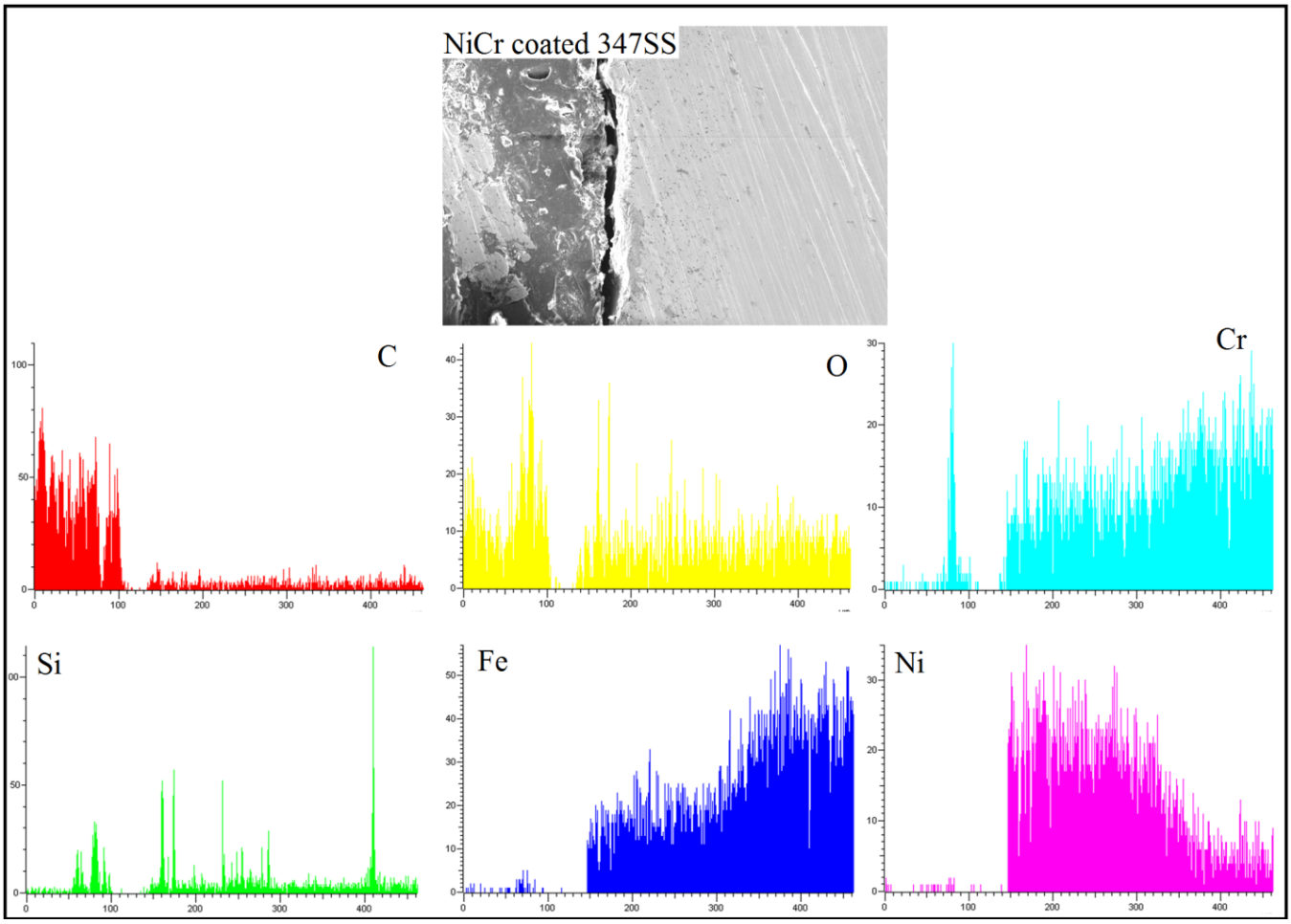

Figure 7.7 X-Ray mapping of 75Ni25Cr coated 347H SS steel after exposed in husk fired boiler for 150 hours at a temperature range between 750±50ºC.

7.1.5 THICKNESS LOSS MEASUREMENTS

The calculation of mpy can also be done as follows: In a year there are 8730 hours and 1mm is equal to 39.37 mils. So, for "z" mm thickness loss for 1000 hours, mpy is (z) × (39.37) × (8760/1000). Fig 7.8 clearly shows than NiCr coated sample was less affected by corrosion as its corrosion rate is considerably less than that of bare 347H SS sample that was hung in husk fired boiler.

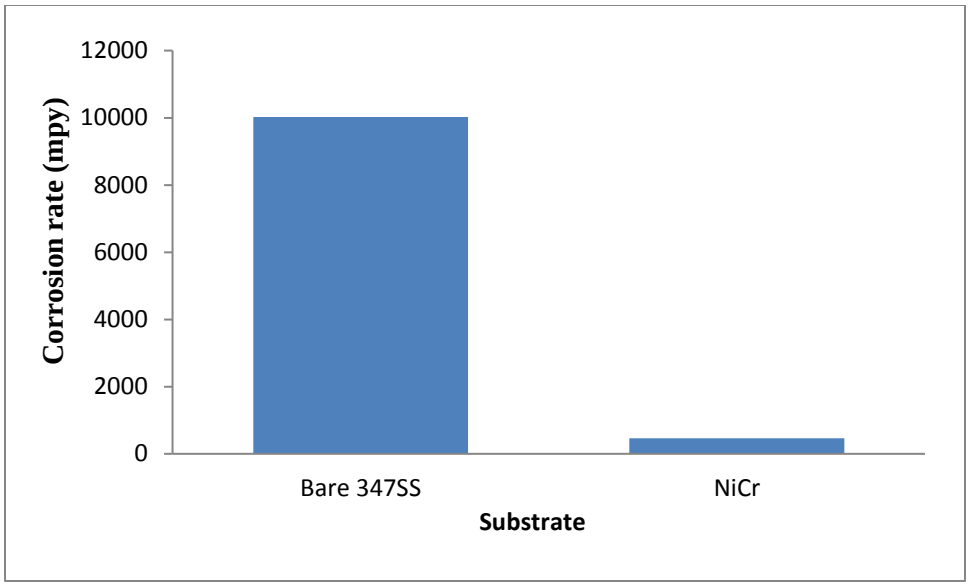

Fig 7.8: Corrosion rate in terms of milli-inches per year

7.2 DISCUSSION

Form visual analysis it can be clearly seen that bare 347H SS was adversely affected by high temperature corrosion phenomenon under the actual boiler environment. While NiCr coated specimen showed better resistance to corrosion in similar harsh environment. XRD analysis shows the presence of Fe_3O_4 oxide and presence of Fe is also shown by X-ray mapping in oxide and metal region for bare sample. As Fe_3O_4 is non protective oxide layer, thus we can conclude that excessive metal loss in bare 347H SS is due to formation of iron oxide which was also reported by (Mudgal et al. 2012). SEM image for bare sample showed the formation of large granular iron oxides. EDS conformed the elements present were mainly Fe and O only. Big cracks were observed which is due to the iron oxide scale which has low thermal coefficient of expansion (Peng et al. 2010).

XRD analysis detected formation of Cr_2O_3 oxide layer in both the samples. This formation of chromium oxide may be because of the affinity of chromium towards oxygen at high temperature (Gupta et al. 2012). In XRD analysis major of NiCr coated sample shows oxides peaks of Fe_2O_3, K_2CrO_4, and spinel $NiCr_2O_4$ (Takeda et al. 2009). Formation of K_2CrO_4 could be explained by presence of potassium in boiler environment which reacts with Cr_2O_3 to form K_2CrO_4 by following reaction.

$$Cr_2O_3(s) + 4KCl(s) + (\frac{5}{2})O_2(g) \rightarrow 2K_2CrO_4(s) + 2Cl_2(g) \quad \text{.....(7.1)}$$

Similarly, $NiCr_2O_4$ oxide was formed after solid state reaction between nickel oxide and chromium oxide. Nickel and chromium is present in the coating which when combine with oxygen formed oxide as shown in equation 7.2.

$NiO + Cr_2O_3 \longrightarrow NiCr_2O_4$ .....(7.2)

The presence of Fe_2O_3 could be explained by following reaction.

$4Fe + 3O_2 \longrightarrow 2Fe_2O_3$

It could be concluded that better protection of NiCr coated specimen was due to the presence of protective oxides of K_2CrO_4 and Cr_2O_3 in oxide layer.

7.3 CONCLUSION

1. The bare and coated 347H SS were subjected to actual husk fired boiler in necter plant Derrabassi Punjab. These samples were exposed for 150 hours in boiler.
2. Both the specimen underwent sever corrosion but NiCr coated specimen showed better resistance to corrosion.
3. Ash deposits was found on the samples which consisted of various sulphates, carbonates and silicates weight measurements was replaced by thickness loss of the substrate or the coating and the corrosion was calculated in terms of mils per year.
4. The better performance of NiCr coated sample may be may be attributed to formation of of chromium oxide .
5. Ash deposits on all the substrates have following constituent: Sodium sulphate, calcium sulphate and magnesium silicate.

CHAPTER 8

FUTURE SCOPE

1. Rare earth/Reactive elements addition should be tried into the coating at different concentration to find out the optimum content for obtaining a desired properties.
2. Stepwise corrosion mechanism should be formulated to understand the mechanism of corrosion in incinerators environment.
3. Superalloys substrate can be taken instead of steel to assess the protective role of the coatings. More study should be done in actual medical waste incinerator environment for longer durations and actual biomass fuel fired boiler.
4. Study of coating thickness of thermal spray coating process using Taguchi method.
5. Study of nano structured coatings under different environment.
6. Developing hydrophobic and super hydrophobic coating.

REFRENCES

1. Anžel I. High temperature oxidation of metals and alloys. Metalurgija. 2007;13(4):325-36.
2. Aho, M., et al. "Reduction of superheater corrosion by co-firing risky biomass with sewage sludge." *Fuel* 89.9 (2010): 2376-2386.
3. Asbury FE, Brooks S. Superheater Tubes for Advanced Coal-fired Power Plant in the UK. ASM International,. 1987:213-8.
4. Baxter L. Biomass-coal co-combustion: opportunity for affordable renewable energy. Fuel. 2005 Jul 31;84(10):1295-302.
5. Blunt J, Balchin NC. Health and safety in welding and allied processes. Woodhead Publishing; 2002.
6. Birks N, Meier GH, Pettit FS. Introduction to the high temperature oxidation of metals. Cambridge University Press; 2006 Mar 30.
7. Bémer D, Régnier R, Subra I, Sutter B, Lecler MT, Morele Y. Ultrafine particles emitted by flame and electric arc guns for thermal spraying of metals. Annals of occupational hygiene. 2010 Aug 1;54(6):607-14.
8. Cornell RM, Schwertmann U. The iron oxides: structure, properties, reactions, occurrences and uses. John Wiley & Sons; 2003 Oct 17.
9. Chatha SS, Sidhu HS, Sidhu BS. The effects of post-treatment on the hot corrosion behavior of the HVOF-sprayed Cr 3 C 2–NiCr coating. Surface and Coatings Technology. 2012 May 25;206(19):4212-24.
10. Davis JR, editor. Handbook of thermal spray technology. ASM international; 2004.
11. Ekuma CE, Idenyi NE. The Inhibition Characteristic of Brine on the Corrosion Susceptibility of Al-Zn Alloy Systems. Applied Sci. 2006 Aug;6:1751-5.
12. Grabke HJ, Reese E, Spiegel M. The effects of chlorides, hydrogen chloride, and sulfur dioxide in the oxidation of steels below deposits. Corrosion science. 1995 Jul 1;37(7):1023-43.

13. Giggins CS, Pettit FS. Corrosion of metals and alloys in mixed gas environments at elevated temperatures. Oxidation of Metals. 1980 Oct 31;14(5):363-413.

14. Gupta OP, Mudgal D, Puri D, Prakash S. High temperature cyclic oxidation of Ni based superalloys at 900 C in air. International Journal of Advanced Scientific Research and Technology. 2012;2(2):486-92.

15. Gurumoorthi G, Rengarajan R, Balaji D, Manikandan C. High Temperature oxidation behavior of materials for super critical fossils fuel Power plant.

16. Grote KH, Antonsson EK. Springer handbook of mechanical engineering. Springer Science & Business Media; 2009 Jan 13.

17. Hussain T, McCartney DG, Shipway PH, Zhang D. Bonding mechanisms in cold spraying: the contributions of metallurgical and mechanical components. Journal of Thermal Spray Technology. 2009 Sep 1;18(3):364-79.

18. Huheey JE, Keiter EA, Keiter RL, Medhi OK. Inorganic chemistry: principles of structure and reactivity. Pearson Education India; 2006.

19. Kuroda S, Kawakita J, Watanabe M, Katanoda H. Warm spraying—a novel coating process based on high-velocity impact of solid particles. Science and technology of advanced materials. 2008 Sep 10;9(3):033002.

20. Kakac, S. Boilers, evaporators, and condensers. John Wiley & Sons. 1991.

21. Kumar DG. *Optimization of Spray Parametrs for High Velocity Oxy-Fuel (HVOF) Sprayed Abradable Coating* (Doctoral dissertation).

22. Kawakita J, Katanoda H, Watanabe M, Yokoyama K, Kuroda S. Warm spraying: an improved spray process to deposit novel coatings. Surface and Coatings Technology. 2008 Jun 15;202(18):4369-73.

23. Knotek O. Thermal spraying and detonation gun processes. Handbook of Hard Coatings Deposition Technologies, Properties and Applications. 2001:77-107

24. Kamal S, Jayaganthan R, Prakash S. Evaluation of cyclic hot corrosion behaviour of detonation gun sprayed Cr 3 C 2–25% NiCr coatings on nickel-and iron-based superalloys. Surface and coatings technology. 2009 Jan 15;203(8):1004-13.

25. Kumar R, Tewari VK, Prakash S. Studies on hot corrosion of the 2.25 Cr-1Mo boiler tube steel and its weldments in the molten salt Na2SO4-60 pct V2O5 environment. Metallurgical and Materials Transactions A. 2007 Jan 1;38(1):54-7.

26. Leroux F, Campagne C, Perwuelz A, Gengembre L. Fluorocarbon nano-coating of polyester fabrics by atmospheric air plasma with aerosol. Applied Surface Science. 2008 Apr 30;254(13):3902-8.

27. Moridi A, Hassani-Gangaraj SM, Guagliano M, Dao M. Cold spray coating: review of material systems and future perspectives. Surface Engineering. 2014 Jun 1;30(6):369-95.

28. Mudgal D, Singh S, Prakash S. High temperature cyclic oxidation behavior of Ni and Co based superalloys. Journal of Minerals and Materials Characterization and Engineering. 2012 Mar 20;11(03):211.

29. Mougin J, Le Bihan T, Lucazeau G. High-pressure study of Cr 2 O 3 obtained by high-temperature oxidation by X-ray diffraction and Raman spectroscopy. Journal of Physics and Chemistry of Solids. 2001 Mar 31;62(3):553-63

30. Meadowcroft DB. High temperature corrosion of alloys and coatings in oil-and coal-fired boilers. Materials Science and Engineering. 1987 Apr 1;88:313-20

31. Mahesh RA, Jayaganthan R, Prakash S. Evaluation of hot corrosion behaviour of HVOF sprayed NiCrAl coating on superalloys at 900 C. Materials Chemistry and Physics. 2008 Oct 15;111(2):524-33.

32. Osgerby S. Oxide scale damage and spallation in P92 martensitic steel. Materials at High Temperatures. 2008 May 1;17(2):307-10..

33. Powell CA, Morreale BD. Materials challenges in advanced coal conversion technologies. Mrs Bulletin. 2008 Apr;33(4):309-15.

34. Paulussen S, Rego R, Goossens O, Vangeneugden D, Rose K. Plasma polymerization of hybrid organic–inorganic monomers in an atmospheric pressure dielectric barrier discharge. Surface and Coatings Technology. 2005 Oct 1;200(1):672-5.

35. Peng H, Guo H, He J, Gong S. Cyclic oxidation and diffusion barrier behaviors of oxides dispersed NiCoCrAlY coatings. Journal of Alloys and Compounds. 2010 Jul 23;502(2):411-6.]

36. Pettersson J, Asteman H, Svensson JE, Johansson LG. KCl induced corrosion of a 304-type austenitic stainless steel at 600 C; the role of potassium. Oxidation of Metals. 2005 Aug 1;64(1):23-41.

37. Rehn IM. Long-term performance of chromate-treated superheater and reheater tubes. Advances in Material Technology for Fossil Power Plants. 1987:297-303.

38. Roberge PR. Corrosion Engineering. New York, NY, USA:: McGraw-Hill; 2008.

39. Simms HG. *Oxidation behaviour of austenitic stainless steels at high temperature in supercritical plant* (Doctoral dissertation, University of Birmingham).2011

40. Sidhu BS, Prakash S. Evaluation of the corrosion behaviour of plasma-sprayed Ni 3 Al coatings on steel in oxidation and molten salt environments at 900 C. Surface and Coatings Technology. 2003 Mar 3;166(1):89-100.

41. Stringer J. Hot corrosion of high-temperature alloys. Annual Review of Materials Science. 1977 Aug;7(1):477-509

42. Singh L, Chawla V, Grewal JS. A review on detonation gun sprayed coatings. JMMCE. 2012 Mar 20;11:243-65..

43. Sidhu, T.S., et al. "Oxidation and hot corrosion resistance of HVOF WC-NiCrFeSiB coating on Ni-and Fe-based superalloys at 800 C." *Journal of Thermal Spray Technology* 16.5-6 (2007): 844-849.

44. Szymański K, Hernas A, Moskal G, Myalska H. Thermally sprayed coatings resistant to erosion and corrosion for power plant boilers-a review. Surface and Coatings Technology. 2015 Apr 25;268:153-64.

45. Tanner CB.Plant temperatures. Agronomy journal. 2008;55(2):210-1.

46. Takeda M, Onishi T, Nakakubo S, Fujimoto S. Physical properties of iron-oxide scales on Si-containing steels at high temperature. Materials transactions. 2009 Sep 1;50(9):2242-6.

47. Viswanathan R, Bakker W. Materials for ultrasupercritical coal power plants—Boiler materials: Part 1. Journal of Materials Engineering and Performance. 2001 Feb 1;10(1):81-95.

48. Watanabe, Shigehiro, Noboru Takubo, and Kanta Kondou. "Water-tube boiler." U.S. Patent No. 6,116,196. 12 Sep. 2000.

49. Weizhong F. Comprehensive Prevention of Steam-Side Scaling and Solid Particle Erosion of Ultra Supercritical Unit. Proceedings of Supercritical Coal: Operating Experience and Technology Developments, I Mech E. 2007.

50. Wang Y, Fei W, An L. Oxidation/Corrosion of Polymer-Derived SiAlCN Ceramics in Water Vapor. Journal of the American Ceramic Society. 2006 Mar 1;89(3):1079-82

51. Xu L, Wang Y, Jing H, Zhao L, Han Y. Deformation Mechanism and Microstructure Evolution of T92/S30432 Dissimilar Welded Joint During Creep. Journal of Materials Engineering and Performance. 2016 Sep 1;25(9):3960-71.

52. Yang CW, Lui TS. Effect of hydrothermal self-healing and intermediate strengthening layers on adhesion reinforcement of plasma-sprayed hydroxyapatite coatings. InAdvanced Plasma Spray Applications 2012. InTech.

53. Zhou W, Zhou K, Deng C, Zeng K, Li Y. Hot corrosion behaviour of HVOF-sprayed Cr 3 C 2-NiCrMoNbAl coating. Surface and Coatings Technology. 2017 Jan 15;309:849-59.

Appendix

Weight change of substrate under cyclic oxidation

Uncoated 347H H substrate

Weight change of Bare 347H H substrate after every cyclic oxidation

WEIGHT OF SAMPLE: 10.700 g					
WEIGHT OF BOAT: 43.553					
WEIGHT OF SAMPLE + BOAT: 54.253					
Cycle	DATE	TIME IN	TIME OUT	WEIGHT (g)	COMMENT
1	30/3	5.13 PM	6:13pm	54.251	Formation of dark Reddish orange oxide with spots of green oxide
2	31/3	10:16am	11:16am	54.250	reddish orange oxide is formed
3	31/3	11:38am	12:38pm	54.253	reddish orange oxide is formed
4	31/3	12:50pm	1:50pm	54.250	reddish colour
5	31/3	2:01pm	3:01pm	54.252	Light grey & dark grey oxide, Reddish orange oxide is formed.
6	31/3	3:25pm	4:25pm	54.254	Spallation &sputtering is observed
7	31/3	4:50pm	5:50pm	54.252	Spallation &sputtering continuous

8	31/3	6:25pm	7:25pm	54.250	dark grey colour oxide with spallation &sputtering
9	1/4	8:44am	9:44pm	54.253	dark grey colour oxide & dark green oxide with increased in spallation
10	1/4	10:15am	11:15pm	54.252	dark grey colour oxide with spallation & green colour oxide
11	1/4	11:45am	12:45pm	54.254	Spallation &sputtering has increased
12	01-Apr	1:20pm	2:22pm	54.253	Dark grey and green colour oxide with increase in spallation and sputtering
13	01-Apr	3:00pm	4:00pm	54.252	Dark grey and green colour oxide with increase in spallation and sputtering
14	01-Apr	4:35pm	5:35pm	54.253	Dark grey and green colour oxide with increase in spallation and sputtering
15	01-Apr	6:00pm	7:00pm	54.254	Dark grey and green colour oxide with increase in spallation and sputtering
16	03-Apr	9:00am	10.00am	54.252	sputtering and spallation increased
17	03-Apr	10:25	11:25	54.254	sputtering and spallation increased
18	03-Apr	12:00	1:00	54.255	no more sputtering and spallation
19	03-Apr	1:35	2:35	54.256	no more sputtering and spallation
20	03-Apr	3:05	4:05	54.253	no more sputtering and spallation

21	03-Apr	4:32	5:32	54.253	no more sputtering and spallation
22	03-Apr	6:00	7:00	59.118	no more sputtering and spallation
23	03-Apr	7:35	8:35	59.122	no more sputtering and spallation
24	04-Apr	8:40am	9:40am	59.123	more sputtering and spallation
25	04-Apr	10:00	11:00	59.119	dark brown & grey colour oxide with more sputtering &spallation
26	04-Apr	11:30	12:30	59.117	dark brown & grey colour oxide with more sputtering &spallation
27	04-Apr	1:00	2:00	59.116	dark green oxide, some spots of grey colour oxide
28	04-Apr	2:25	3:25	59.118	grey colour oxide & green with more sputtering& colour spallation
29	04-Apr	4:00	5:00	59.115	grey colour oxide & green with more sputtering& colour spallation
30	04-Apr	5:30	06:30	59.116	grey colour oxide & green with more sputtering& colour spallation
31	04-Apr	7:00	8:00	59.119	grey colour oxide & green with more sputtering& colour spallation
32	05-Apr	09:00am	10:00am	59.119	grey colour oxide & green with more sputtering& colour spallation

33	05-Apr	10:30	11:30	59.117	grey colour oxide & green with more sputtering& colour spallation
34	05-Apr	12:00	1:00	59.117	grey colour oxide & green with more sputtering & colour spallation
35	05-Apr	1:30	2:30	59.118	grey colour oxide & green with more sputtering& colour spallation
36	05-Apr	3:00	4:00	59.118	grey colour oxide & green with more sputtering& colour spallation
37	05-Apr	4:30	5:30	59.119	grey colour oxide & green with more sputtering& colour spallation
38	05-Apr	6:00	7:00	59.118	grey colour oxide & green with more sputtering& colour spallation
39	06-Apr	8:25am	9:25am	59.114	grey colour oxide & green with more sputtering& colour spallation
40	06-Apr	9:55am	10:55	59.118	grey colour oxide & green with more sputtering& colour spallation
41	06-Apr	11:30	12:30	59.114	grey colour oxide & green with more sputtering& colour spallation
42	06-Apr	1:00	2:00	59.116	grey colour oxide & green with more sputtering& colour spallation
43	06-Apr	2:30	3:30	59.115	grey colour oxide & green with more sputtering& colour spallation

44	06-Apr	4:00	5:00	59.115	grey colour oxide & green with more sputtering& colour spallation
45	06-Apr	5:30	6:30	59.114	grey colour oxide & green with more sputtering& colour spallation
46	07-Apr	9:00am	10:00am	59.113	grey colour oxide & green with more sputtering& colour spallation
47	07-Apr	10:30	11:30	59.113	grey colour oxide & green with more sputtering& colour spallation
48	07-Apr	12:00	1:00	59.114	grey colour oxide & green with more sputtering& colour spallation
49	07-Apr	1:30	2:30	59.114	grey colour oxide & green with more sputtering& colour spallation
50	07-Apr	3:00	4:00	59.119	grey colour oxide & green with more sputtering& colour spallation

Weight change of substrate under cyclic oxidation

NiCr coated 347H H substrate

Weight change of NiCr 347H H substrate after every cyclic oxidation

WEIGHT OF SAMPLE: 11.899 g					
WEIGHT OF BOAT: 44.599					
WEIGHT OF SAMPLE + BOAT: 56.498					
Cycle	DATE	TIME IN	TIME OUT	WEIGHT (g)	COMMENT
1	30/3	5.13 PM	6:13pm	56.500	Formation of dark Reddish orange oxide with spots of green oxide
2	31/3	10:16am	11:16am	56.501	reddish orange oxide is formed
3	31/3	11:38am	12:38pm	56.501	reddish orange oxide is formed
4	31/3	12:50pm	1:50pm	56.499	reddish orange, grey brown colour oxide is formed ; spallation is also observed.
5	31/3	2:01pm	3:01pm	56.499	Light grey & dark grey oxide, Reddish orange oxide is formed. Spallation is also observed.
6	31/3	3:25pm	4:25pm	56.498	Spallation &sputtering is observed. Dark brown & grey colour oxide is observed.
7	31/3	4:50pm	5:50pm	56.498	dark grey colour oxide with spots of brown colour oxide. Spallation &sputteringcontinuous
8	31/3	6:25pm	7:25pm	56.504	dark grey colour oxide with spallation &sputtering

9	1/4	8:44am	9:44pm	56.500	dark grey colour oxide & dark green oxide with increased in spallation
10	1/4	10:15am	11:15pm	56.499	dark grey colour oxide with spallation & green colour oxide
11	1/4	11:45am	12:45pm	56.500	Spallation &sputtering has increased
12	01-Apr	1:20pm	2:22pm	56.499	increase in spallation and sputtering
13	01-Apr	3:00pm	4:00pm	59.499	spallation and sputtering
14	01-Apr	4:35pm	5:35pm	56.500	Dark grey and green colour oxide with increase in spallation and sputtering
15	01-Apr	6:00pm	7:00pm	56.501	Dark grey and green colour oxide with increase in spallation and sputtering
16	03-Apr	9:00am	10.00am	56.498	sputtering and spallation increased
17	03-Apr	10:25	11:25	56.499	sputtering and spallation increased
18	03-Apr	12:00	1:00	56.500	no more sputtering and spallation
19	03-Apr	1:35	2:35	56.501	no more sputtering and spallation
20	03-Apr	3:05	4:05	56.501	no more sputtering and spallation
21	03-Apr	4:32	5:32	56.501	no more sputtering and spallation

22	03-Apr	6:00	7:00	56.501	no more sputtering and spallation
23	03-Apr	7:35	8:35	56.500	no more sputtering and spallation
24	04-Apr	8:40am	9:40am	56.500	more sputtering and spallation
25	04-Apr	10:00	11:00	56.499	dark brown & grey colour oxide with more sputtering &spallation
26	04-Apr	11:30	12:30	56.498	dark brown & grey colour oxide with more sputtering &spallation
27	04-Apr	1:00	2:00	56.498	dark green oxide, some spots of grey colour oxide
28	04-Apr	2:25	3:25	56.499	grey colour oxide & green with more sputtering& colour spallation
29	04-Apr	4:00	5:00	56.499	grey colour oxide & green with more sputtering& colour spallation
30	04-Apr	5:30	06:30	56.500	grey colour oxide & green with more sputtering& colour spallation
31	04-Apr	7:00	8:00	56.501	grey colour oxide & green with more sputtering& colour spallation
32	05-Apr	09:00am	10:00am	56.502	grey colour oxide & green with more sputtering& colour spallation
33	05-Apr	10:30	11:30	56.499	grey colour oxide & green with more sputtering& colour spallation

34	05-Apr	12:00	1:00	56.499	grey colour oxide & green with more sputtering & colour spallation
35	05-Apr	1:30	2:30	56.501	grey colour oxide & green with more sputtering& colour spallation
36	05-Apr	3:00	4:00	56.501	grey colour oxide & green with more sputtering& colour spallation
37	05-Apr	4:30	5:30	56.501	grey colour oxide & green with more sputtering& colour spallation
38	05-Apr	6:00	7:00	56.501	grey colour oxide & green with more sputtering& colour spallation
39	06-Apr	8:25am	9:25am	56.496	grey colour oxide & green with more sputtering& colour spallation
40	06-Apr	9:55am	10:55	56.501	grey colour oxide & green with more sputtering& colour spallation
41	06-Apr	11:30	12:30	56.500	grey colour oxide & green with more sputtering& colour spallation
42	06-Apr	1:00	2:00	56.501	grey colour oxide & green with more sputtering& colour spallation
43	06-Apr	2:30	3:30	56.500	grey colour oxide & green with more sputtering& colour spallation
44	06-Apr	4:00	5:00	56.500	grey colour oxide & green with more sputtering& colour spallation

45	06-Apr	5:30	6:30	56.500	grey colour oxide & green with more sputtering& colour spallation
46	07-Apr	9:00am	10:00am	56.505	grey colour oxide & green with more sputtering& colour spallation
47	07-Apr	10:30	11:30	56.504	grey colour oxide & green with more sputtering& colour spallation
48	07-Apr	12:00	1:00	56.498	grey colour oxide & green with more sputtering& colour spallation
49	07-Apr	1:30	2:30	56.500	grey colour oxide & green with more sputtering& colour spallation
50	07-Apr	3:00	4:00	56.501	grey colour oxide & green with more sputtering& colour spallation

Weight change of substrate under cyclic oxidation

Uncoated 347H H substrate

Weight change of bare 347H H substrate after every cyclic hot corrosion

WEIGHT OF SAMPLE: 11.938 g					
WEIGHT OF BOAT: 42.170 g					
WEIGHT OF SAMPLE + BOAT: 54.095					
Cycle	DATE	TIME IN	TIME OUT	WEIGHT (g)	COMMENT
1	10 Apr	3:37 PM	4:37pm	54.107	Formation of dark Reddish orange oxide with spots of green oxide
2	11 Apr	9:16am	10:16am	54.116	reddish orange oxide is formed
3	11 Apr	10:45am	11:45pm	54.100	reddish orange oxide is formed
4	11 Apr	12:20pm	1:20pm	54.086	reddish orange, grey brown colour oxide is formed
5	11 Apr	1:50pm	2:50pm	54.092	Light grey & dark grey oxide, Reddish orange oxide is formed.
6	11 Apr	3:25pm	4:25pm	54.093	Dark brown & grey colour.
7	11 Apr	4:50pm	5:50pm	54.094	dark grey colour oxide with spots of brown colour oxide.

8	11 Apr	6:25pm	7:25pm	54.093	dark grey colour oxide with spallation &sputtering
9	12 Apr	9:05am	10:05pm	54.090	dark grey colour oxide
10	12 Apr	10:30am	11:30pm	54.092	dark grey colour oxide with spallation & green colour oxide
11	12 Apr	12:00am	1:00pm	54.093	Spallation &sputtering has increased
12	12-Apr	1:30pm	2:30pm	54.090	Dark grey and green colour oxide with increase in spallation and sputtering
13	12-Apr	3:00pm	4:00pm	54.088	Dark grey and green colour oxide with increase in spallation and sputtering
14	12-Apr	4:35pm	5:35pm	54.090	Dark grey and green colour oxide with increase in spallation and sputtering
15	12-Apr	6:00pm	7:00pm	54.090	Dark grey and green colour oxide with increase in spallation and sputtering
16	13-Apr	9:00am	10.00am	54.090	sputtering and spallation increased
17	13-Apr	9:15	10:15	54.089	sputtering and spallation increased
18	13-Apr	10:45	11:45	54.088	no more sputtering and spallation
19	13-Apr	12:10	1:10	54.087	no more sputtering and spallation
20	13-Apr	1:45	2:45	54.084	no more sputtering and spallation

21	13-Apr	3:20	4:20	54.086	no more sputtering and spallation
22	13-Apr	4:45	5:45	54.084	no more sputtering and spallation
23	14-Apr	9:35	10:35	54.081	no more sputtering and spallation
24	14-Apr	11:00am	12:00am	54.084	more sputtering and spallation
25	14-Apr	12:30	1:30	54.085	dark brown & grey colour oxide with more sputtering &spallation
26	14-Apr	2:00	3:00	54.083	dark brown & grey colour oxide with more sputtering &spallation
27	14-Apr	3:30	4:30	54.076	dark green oxide, some spots of grey colour oxide
28	14-Apr	5:00	6:00	54.085	grey colour oxide & green with more sputtering& colour spallation
29	14-Apr	4:00	5:00	54.084	grey colour oxide & green with more sputtering& colour spallation
30	14-Apr	6:30	7:30	54.107	grey colour oxide & green with more sputtering& colour spallation
31	15-Apr	9:20	10:20	54.104	grey colour oxide & green with more sputtering& colour spallation
32	15-Apr	10:50am	11:50am	54.101	grey colour oxide & green with more sputtering& colour spallation

33	15-Apr	12:20	1:20	54.099	grey colour oxide & green with more sputtering& colour spallation
34	15-Apr	1:45	2:45	54.099	grey colour oxide & green with more sputtering & colour spallation
35	15-Apr	3:30	4:30	54.099	grey colour oxide & green with more sputtering& colour spallation
36	15-Apr	5:00	6:00	54.099	grey colour oxide & green with more sputtering& colour spallation
37	17-Apr	9:10	10:10	54.100	grey colour oxide & green with more sputtering& colour spallation
38	17-Apr	10:40	11:40	54.100	grey colour oxide & green with more sputtering& colour spallation
39	17-Apr	11:05am	1:05pm	54.101	grey colour oxide & green with more sputtering& colour spallation
40	17-Apr	1:30am	2:30	54.102	grey colour oxide & green with more sputtering& colour spallation
41	17-Apr	3:00	4:00	54.100	grey colour oxide & green with more sputtering& colour spallation
42	17-Apr	4:30	5:30	54.097	grey colour oxide & green with more sputtering& colour spallation
43	17-Apr	6:00	7:00	54.097	grey colour oxide & green with more sputtering& colour spallation

44	18-Apr	9:40	10:40	54.097	grey colour oxide & green with more sputtering& colour spallation
45	18-Apr	11:10	12:10	54.096	grey colour oxide & green with more sputtering& colour spallation
46	18-Apr	12:40am	1:40am	54.096	grey colour oxide & green with more sputtering& colour spallation
47	18-Apr	2:10	3:10	54.097	grey colour oxide & green with more sputtering& colour spallation
48	18-Apr	3:40	4:40	54.097	grey colour oxide & green with more sputtering& colour spallation
49	18-Apr	5:10	6:10	54.097	grey colour oxide & green with more sputtering& colour spallation
50	18-Apr	6:40	7:40	54.096	grey colour oxide & green with more sputtering& colour spallation

Weight change of substrate under cyclic oxidation

NiCr coated substrate

Weight change of NiCr substrate after every cyclic hot corrosion

WEIGHT OF SAMPLE: 12.966 g					
WEIGHT OF BOAT: 44.593 g					
WEIGHT OF SAMPLE + BOAT: 57.562 g					
Cycle	DATE	TIME IN	TIME OUT	WEIGHT (g)	COMMENT
1	10 Apr	3:37 PM	4:37pm	57.564	Formation of dark Reddish orange oxide with spots of green oxide
2	11 Apr	9:16am	10:16am	57.566	reddish orange oxide is formed
3	11 Apr	10:45am	11:45pm	57.567	reddish orange oxide is formed
4	11 Apr	12:20pm	1:20pm	57.567	reddish orange, grey brown colour oxide is formed ; spallation is also observed.
5	11 Apr	1:50pm	2:50pm	57.569	Light grey & dark grey oxide, Reddish orange oxide is formed. Spallation is also observed.
6	11 Apr	3:25pm	4:25pm	57.568	Spallation &sputtering is observed. Dark brown & grey colour oxide is observed.
7	11 Apr	4:50pm	5:50pm	57.569	dark grey colour oxide with spots of brown colour oxide. Spallation &sputteringcontinuous
8	11 Apr	6:25pm	7:25pm	57.568	dark grey colour oxide with spallation &sputtering

9	12 Apr	9:05am	10:05pm	57.568	dark grey colour oxide & dark green oxide with increased in spallation
10	12 Apr	10:30am	11:30pm	57.569	dark grey colour oxide with spallation & green colour oxide
11	12 Apr	12:00am	1:00pm	57.568	Spallation &sputtering has increased
12	12-Apr	1:30pm	2:30pm	57.569	Dark grey and green colour oxide with increase in spallation and sputtering
13	12-Apr	3:00pm	4:00pm	57.568	Dark grey and green colour oxide with increase in spallation and sputtering
14	12-Apr	4:35pm	5:35pm	57.569	Dark grey and green colour oxide with increase in spallation and sputtering
15	12-Apr	6:00pm	7:00pm	57.570	Dark grey and green colour oxide with increase in spallation and sputtering
16	13-Apr	9:00am	10.00am	57.566	sputtering and spallation increased
17	13-Apr	9:15	10:15	57.568	sputtering and spallation increased
18	13-Apr	10:45	11:45	57.566	no more sputtering and spallation
19	13-Apr	12:10	1:10	57.565	no more sputtering and spallation
20	13-Apr	1:45	2:45	57.564	no more sputtering and spallation
21	13-Apr	3:20	4:20	57.566	no more sputtering and spallation

22	13-Apr	4:45	5:45	57.564	no more sputtering and spallation
23	14-Apr	9:35	10:35	57.66	no more sputtering and spallation
24	14-Apr	11:00am	12:00am	57.564	more sputtering and spallation
25	14-Apr	12:30	1:30	57.564	dark brown & grey colour oxide with more sputtering &spallation
26	14-Apr	2:00	3:00	57.563	dark brown & grey colour oxide with more sputtering &spallation
27	14-Apr	3:30	4:30	57.562	dark green oxide, some spots of grey colour oxide
28	14-Apr	5:00	6:00	57.563	grey colour oxide & green with more sputtering& colour spallation
29	14-Apr	4:00	5:00	57.563	grey colour oxide & green with more sputtering& colour spallation
30	14-Apr	6:30	7:30	57.579	grey colour oxide & green with more sputtering& colour spallation
31	15-Apr	9:20	10:20	57.590	grey colour oxide & green with more sputtering& colour spallation
32	15-Apr	10:50am	11:50am	57.580	grey colour oxide & green with more sputtering& colour spallation
33	15-Apr	12:20	1:20	57.591	grey colour oxide & green with more sputtering& colour spallation

34	15-Apr	1:45	2:45	57.575	grey colour oxide & green with more sputtering & colour spallation
35	15-Apr	3:30	4:30	57.566	grey colour oxide & green with more sputtering& colour spallation
36	15-Apr	5:00	6:00	55.566	grey colour oxide & green with more sputtering& colour spallation
37	17-Apr	9:10	10:10	57.576	grey colour oxide & green with more sputtering& colour spallation
38	17-Apr	10:40	11:40	57.577	grey colour oxide & green with more sputtering& colour spallation
39	17-Apr	11:05am	1:05pm	57.577	grey colour oxide & green with more sputtering& colour spallation
40	17-Apr	1:30am	2:30	57.577	grey colour oxide & green with more sputtering& colour spallation
41	17-Apr	3:00	4:00	57.576	grey colour oxide & green with more sputtering& colour spallation
42	17-Apr	4:30	5:30	57.575	grey colour oxide & green with more sputtering& colour spallation
43	17-Apr	6:00	7:00	57.576	grey colour oxide & green with more sputtering& colour spallation
44	18-Apr	9:40	10:40	57.574	grey colour oxide & green with more sputtering& colour spallation

45	18-Apr	11:10	12:10	57.574	grey colour oxide & green with more sputtering& colour spallation
46	18-Apr	12:40am	1:40am	57.574	grey colour oxide & green with more sputtering& colour spallation
47	18-Apr	2:10	3:10	57.575	grey colour oxide & green with more sputtering& colour spallation
48	18-Apr	3:40	4:40	57.576	grey colour oxide & green with more sputtering& colour spallation
49	18-Apr	5:10	6:10	57.575	grey colour oxide & green with more sputtering& colour spallation
50	18-Apr	6:40	7:40	57.575	grey colour oxide & green with more sputtering& colour spallation